JOURNAL OF MORPHOLOGY 185:297-326 (1985)

Functional Morphology of the Feeding Mechanism in Aquatic Ambystomatid Salamanders

GEORGE V. LAUDER AND H. BRADLEY SHAFFER
Department of Anatomy (G.V.L.) and Committee on Evolutionary Biology (G.V.L., H.B.S.), University of Chicago, Chicago, Illinois 60637

ABSTRACT This study addresses four questions in vertebrate functional morphology through a study of aquatic prey capture in ambystomatid salamanders: 1) How does the feeding mechanism of aquatic salamanders function as a biomechanical system? 2) How similar are the biomechanics of suction feeding in aquatic salamanders and ray-finned fishes? 3) What quantitative relationship does information extracted from electromyograms of striated muscles bear to kinematic patterns and animal performance? and 4) What are the major structural and functional patterns in the evolution of the lower vertebrate skull?

During prey capture, larval ambystomatid salamanders display a kinematic pattern similar to that of other lower vertebrates, with peak gape occurring prior to both peak hyoid depression and peak cranial elevation. The depressor mandibulae, rectus cervicis, epaxialis, hypaxialis, and branchiohyoideus muscles are all active for 40–60 msec during the strike and overlap considerably in activity. The two divisions of the adductor mandibulae are active in a continuous burst for 110–130 msec, and the intermandibularis posterior and coracomandibularis are active in a double burst pattern. The antagonistic depressor mandibulae and adductor mandibulae internus become active within 0.2 msec of each other, but the two muscles show very different spike and amplitude patterns during their respective activity periods. Coefficients of variation for kinematic and most electromyographic recordings reach a minimum within a 10 msec time period, just after the mouth starts to open.

Pressure within the buccal cavity during the strike reaches a minimum of −25 mmHg, and minimum pressure occurs synchronously with maximum gill bar adduction. The gill bars (bearing gill rakers that interlock with rakers of adjacent arches) clearly function as a resistance within the oral cavity and restrict posterior water influx during mouth opening, creating a unidirectional flow during feeding.

Durations of electromyographic activity alone are poor predictors of kinematic patterns. Analyses of spike amplitude explain an additional fraction of the variance in jaw kinematics, whereas the product of spike number and amplitude is the best statistical predictor of kinematic response variables.

Larval ambystomatid salamanders retain the two primitive biomechanical systems for opening and closing the mouth present in nontetrapod vertebrates: elevation of the head by the epaxialis and depression of the mandible by the hyoid apparatus.

During the last half of the nineteenth and at the start of the twentieth century, the key area of active research in morphology concerned the homologies of structural systems in various taxa and patterns of structure as possible indicators of phylogenetic relationship. Morphologists interested in the evolution of the vertebrate skull exemplified this approach, as the work of Allis ('17), Edgeworth ('11), Gaupp ('04), Luther ('14) and Vetter (1874) demonstrates. Although the approach taken by these early investigators

continues to be fruitful today, vertebrate morphology in the last 20 years has focused increasingly on the function of structures and on problems associated with the evolution and mechanics of complex biological designs.

One area of particular interest has been the origin and evolution of the vertebrate feeding mechanism (e.g., Bramble and Wake, '85; Crompton and Parker, '78; Gans and Northcutt, '83; Mallatt, '84a,b). Over the last 5 years, sufficiently detailed analyses of skull structure and function in most of the major lower vertebrate clades have been published to provide a basis for generalizations about the evolution of the lower vertebrate skull. Those groups for which adequate biomechanical research is available include ray-finned fishes (Actinoptergyii; Lauder, '80a,'82, coelacanths (Actinistia; Lauder, '80b); lungfishes (Dipnoi; Bemis and Lauder, '85); and amphibians (Bemis et al., '83; Dalrymple et al., '85; Erdman and Cundall, '84; Larson and Guthrie, '75; Lombard and Wake, '76,'77; Roth, '76; Wake, '82). Current generalizations concerning the evolution of aquatic feeding (such as the proposed role of the hyoid apparatus) are limited in their generality, however, because of a lack of information on three key groups: sharks, aquatic salamanders, and aquatic turtles. Aquatic salamanders are of special importance because any proposals concerning early tetrapod skull function and the origin of terrestrial feeding must be constrained by our understanding of form-function relationships in those living taxa that retain characteristics of early tetrapods. Thus the first goal of this paper is to analyze the functional morphology of aquatic prey capture in ambystomatid salamander larvae to provide data comparable to that available on other lower vertebrate clades.

A second goal of this paper is to evaluate specifically the applicability of biomechanical models proposed for skull function in ray-finned fishes to aquatic salamanders. Salamanders lack a bony operculum that covers the gills laterally, and larval ambystomatid salamanders lack the lateral movement of the palatoquadrate that is found in many ray-finned fishes. The operculum of fishes has been implicated as a crucial component in some models of suction feeding in fishes, and an investigation of skull function in aquatic salamanders affords an opportunity to test by comparative methods the models of prey capture. A specific aim is to evaluate the role of the branchial apparatus as a resistance inside the oral cavity. The gill bars have shown to be a key component of the suction feeding mechanism in fishes (Lauder, '83a), and, if the basic hydrodynamics of suction feeding in salamanders are similar to those of fishes, then a similar function of the gill apparatus is predicted.

The third goal of this paper concerns the evaluation of quantitative analytical methods for electromyographic data. Electromyographic recordings have proven to be an extremely useful tool in the study of vertebrate musculoskeletal systems and in the evaluation of models of skull function (Gans and Gorniak, '82). However, many elaborate functional analyses contain no statistical support for conclusions and only arbitrary determinations of myogram amplitude and its functional significance. In contrast, Weijs and Dantuma ('81), Gorniak et al. ('82), and Gans and Gorniak ('82) suggest specific quantitative procedures that might increase the information that can be extracted from electromyograms. In this paper we use multiple regression techniques to evaluate the efficacy of three different methods of analyzing electromyograms in predicting the movement pattern of ambystomatid salamanders.

Our final goal is to use these data on larval ambystomatids to reconsider the major structural and functional patterns in vertebrate skull evolution.

MATERIALS AND METHODS

Specimens and morphology

Four species were used for both morphological and experimental analyses: *Ambystoma tigrinum* (two individuals), *A. mexicanum* (ten individuals), *A. dumerilii* (two individuals), and *A. ordinarium* (one individual). *A. tigrinum*, *dumerilii*, and *ordinarium* were collected in the field (see Shaffer, '84, for localities), and the *A. mexicanum* were obtained from the Indiana University axolotl colony. Additional specimens from the same locations were used for dissection and clearing and staining for bone and cartilage following the procedure of Dingerkus and Uhler ('77).

All salamanders were sexually mature adults and were maintained in individual 35-liter aquaria at 17°C. Animals used for experiments ranged from 8.3 to 15.5 cm in snout-vent length. Earthworms cut into approximately 1-cm-long pieces were used as food and these pieces were dropped in front of the mouth from above the salamander.

This feeding procedure follows that used previously (Shaffer and Lauder, '85a).

Gross morphological features of the head were studied by dissection using a Zeiss IVB dissecting microscope. A camera lucida was used to illustrate the dissected specimens and cleared and stained material. The nomenclature of certain bones and muscles in the head of urodeles is a matter of some controversy, and the terms chosen were based on 1) previous research by Druner ('01), Larson and Guthrie ('75), Luther ('14), Piatt ('38, '39, '40), and Ozeti and Wake ('69) and 2) the topography of the cranial muscles and bones in comparison to the musculature of nontetrapods such as *Polypterus* and lungfishes. Thus we follow Druner ('01) in calling the major structural elements of the branchial basket *ceratobranchials* (see Fig. 5), because in all nontetrapod vertebrates the endoskeletal elements of the branchial basket that abut the median (unpaired) cartilages are called *hypobranchials* and the next distal elements *ceratobranchials*. It should be emphasized that at present there is no firm guide to disputed homologies in larval amphibians, although comparisons to more primitive clades are usually instructive. Marche and Durand ('83) have recently provided a comparative analysis of gill arch morphology and use the terminology adopted here.

Experimental techniques

Electromyography and cinematography

Electromyographic data were gathered in a fashion identical to that described previously (Lauder, '83b; Shaffer and Lauder, '85a). Bipolar stainless steel electrodes (0.051 mm in diameter) were implanted percutaneously into from six to eight cranial muscles while the animal was under anaesthesia induced by tricaine methane sulfonate. Bared electrode tips were 0.5 mm long. The bared tips of the electrodes were 1.0 mm apart within the muscle belly. A constant electrode insertion procedure was used between experiments to ensure that electrode placement within the muscle was similar. In every case, the electrode wires were inserted along the fiber direction of the muscle. For example, insertion into the depressor mandibulae muscle was made at the posteroventral corner of the lower jaw, and the needle passed posterodorsally into the muscle. As the electrode tips lie at approximately a 20° angle to the axis of the needle as it is inserted, the actual tips will be at a similar angle to the direction of the muscle fibers within the muscle. Similar procedures were followed for the other muscles. Individual electrode pairs were usually sutured to the skin at the point of emergence from the muscle and were attached to the back of the animal with another suture. The signals were amplified 5,000–10,000 times, and the amplifier bandwidth (Grass P511J) was 100–3,000 Hz. Electromyograms were recorded on a Bell and Howell tape recorder and played back on a Gould 260 chart recorder at a speed 15 times slower than that used for recording. (Chart recorder speed was 125 mm/sec to allow bursts of activity to be resolved into individual spike trains.)

A quantitative analysis of the variation of electromyograms between species, individuals, and experimental days is presented elsewhere (Shaffer and Lauder, '85a). In that study, we found no differences in the activity patterns from multiple electrodes within one muscle (exactly 0% of the variation within a muscle was among electrode variance; Shaffer and Lauder, '85a; Table 5). A total of 216 successful feedings were used for the analysis of muscle activity patterns.

Electromyographic recordings of 35 additional successful feedings were synchronized with films taken at 200 frames per sec. A digital pulse generator was used to place a coded pulse on the tape recorder and a simultaneous light dot on the film. Pulses were coded so that extended sequences could be rapidly correlated without the necessity of counting large numbers of individual pulses. An illustrative sample of such synchronized data is presented in Figure 13. Kodak 4X Reversal film was used in conjunction with two 600-Watt Smith-Victor filming lights and a Photosonics 16-1PL high-speed camera.

Pressure recordings

Water pressure was measured within the buccal cavity with a Millar PC-350 catheter-tipped pressure transducer. This transducer has a frequency response of up to 10 KHz in water. A 5-cm length of flexible polyethylene tubing (0.86 mm i.d.) was implanted through the anterior portion of the frontal bones near the midline, and the flanged end of the cannula was pulled flush with the roof of the mouth. The cannula insertion site was chosen to correspond to the location of similar pressure measurements made in ray-finned fishes and to provide maximal stability for the transducer. Recordings made from ray-

finned fishes (in which the pressure drop is much greater) simultaneously in the anterior and posterior regions of the buccal cavity show no statistically significant differences between the pressure magnitudes at the two sites (Lauder, '85). A small clamp was attached around the cannula and fitted snugly against the top of the head to prevent cannula movement. The Millar transducer was threaded down this cannula so that the tip of the transducer was within 1 cm of the mouth cavity. The end of the cannula was then sealed with silicone to prevent movement of the transducer. Pressure recordings always were made simultaneously with electromyograms and impedance measurements.

Impedance recordings

The distance of mouth opening and the distance between adjacent gill bars (ceratobranchials) was transduced using a commercially available (Biocom) impedance converter. Representative traces are illustrated in Figure 16. By implanting unipolar electrodes (bared tip length 1 mm) on each side of an opening between two structures, and by passing a signal (75 kHz, AC) from one electrode to the other, the distance between the sites can be transduced. This procedure is particularly useful for measuring distances between bones that are located inside the head and are too small to be resolved using high-speed x-ray films. An additional benefit of this approach is that distances between points on the head can be transduced directly without the labor of high-speed filming and the concomitant film analysis. Simultaneous measurement of gape profiles from high-speed films and impedance traces confirmed the accuracy of the impedance technique in transducing movements.

Data analysis: Variables and techniques

Films of feeding behavior were analyzed using frame-by-frame projections onto a digitizer (Houston Instruments). Each frame of the strike (usually about 30 frames were measured per feeding) was projected onto the digitizer and three variables measured (Shaffer and Lauder, '85b): hyoid depression (in cm), gape (the distance between the upper and lower jaws in cm), and cranial elevation on the vertebral column (in degrees). From plots of these three variables versus time, four more variables were measured (all in msec): time to maximum hyoid depression, time to maximum gape, time to peak cranial elevation, and the duration of feeding (gape cycle time). Thus a total of seven kinematic variables were measured from films. The graphs of head movements were synchronized with electromyographic recordings by beginning the frame-by-frame analysis at the frame corresponding to the synchronizer pulse that just preceded the first electromyographic activity.

Myograms used for computer analyses were digitized from the tape recorder using a DAS 12-bit A/D converter (sample rate 3,388 Hz per channel) and an IBM XT computer. Several analytical approaches were used. First, the procedure of Beach et al. ('82) and Gorniak et al. ('82) was used, modified slightly so that the output from the computer program used to analyze the myograms provided several variables: the number of spikes per bin interval, the frequency of the spikes, the mean amplitude of the spikes, the mean spike amplitude times spike frequency, and the mean amplitude multiplied by the number of spikes. Spike peaks were identified using the exact same algorithm as Beach et al. ('82): both positive and negative peaks were used and the computer algorithm allowed subtraction of the baseline "noise" level, tracking of the slope of peaks, and detection of a peak by a slope reversal (Beach et al., '82, p. 613). Electromyograms were synchronized with the films by starting the analysis at the synchronization pulse corresponding to that used for the film analysis and by setting the bin width of the myogram analyses to equal the time between frames on the film (5 msec). For both the "spike number times amplitude" and the "mean spike amplitude" analyses from each myogram, several variables were measured: peak voltage or peak spike number times amplitude, the time between peak values in different muscles, and the time from the start of activity in a reference muscle to the peak amplitude of activity in another muscle.

To obtain an average picture of the pattern of amplitude variation in myograms during feeding, kinematic and spike patterns (recorded simultaneously) were averaged for 20 feedings and the mean, standard deviation, standard error, and coefficient of variation were recorded for each bin interval.

An overall summary of the durations of electrical activity in ten cranial muscles was obtained by digitizing the onsets and offsets of muscle activity relative to the onset of a reference muscle, the depressor mandibulae

(see Fig. 14). Mean durations and the standard errors of onsets and offsets are calculated and presented in a standard bar diagram (e.g., Lauder, '83b). Twenty-three variables were measured from the myograms: the relative onset of each muscle (and each burst when a given muscle displayed more than one burst) with respect to the depressor mandibulae and the duration of activity in each burst of each muscle.

The variable abbreviations used in Tables 1–4 have the following meanings: Variables indicated by a muscle abbreviation alone (e.g., DM or AMI) indicate the duration of electrical activity in that muscle; variables with two muscle abbreviations separated by a hyphen indicate the relative time of onset of activity in those two muscles (e.g., DM-RC or DM-AMI).

Four variables were measured from the pressure recordings for each feeding using a digitizer: the duration of the negative pressure pulse, the time to peak negative pressure, maximum negative pressure, and the area under the pressure trace. The last variable was measured because the integral of force (or pressure in this study) over the time it acts is the *impulse* of the force (Rouse, '78) and is equal to the change in momentum of the body on which the force acts (in this case, the water). This variable thus provides a rough measure of the energy the salamander is putting into the water to accelerate the volume of water containing the prey into the mouth, and is an excellent single descriptor of the coordinated work of all cranial muscles and bone movements.

Finally, three variables were digitized from the impedance recordings of gill bar distance: maximum gill bar adduction, the time to peak gill bar adduction, and the time to maximum gill bar abduction.

Statistical procedures

The statistical procedures used in this paper (analysis of variance, least-squares regression, Wilcoxon sign-ranks test, paired t tests, multiple regression) generally follow Sokal and Rohlf ('81) and Siegel ('56).

Multiple regressions were performed on two different data sets. First, a set of multiple regressions was conducted to assess the ability of onset and offset muscle variables to predict variation in buccal pressure and gill bar impedance. As only the onset and offset (and thus the relative timing) of muscle activity was measured for these regressions, no information about EMG amplitude was used. These regressions test the utility of pressure measurements as an index of feeding performance and produce a quantitative assessment of the importance of gill bar adduction in the feeding mechanism.

The concept of a statistical model is critical to understanding the analyses presented in this paper. Statistical models of the form used here are linear. A number of independent variables (such as the duration of EMG activity in four different muscles) are used in linear combination to predict the value of a dependent variable (such as maximum negative pressure in the buccal cavity). Several models can be constructed using different independent variables to ask which linear combination of variables best predicts variation among feedings in pressure. Thus, in Table 4, the "rectus cervicis" model uses only the duration of activity in the rectus cervicis muscle (RC) as a variable in an attempt to predict variation in pressure. Each model has a constant (represented by the symbol b_0 in Table 4) as well as a coefficient for each variable.

Second, three different methods of analyzing electromyograms were compared for their ability to predict variation in the pattern of synchronously recorded kinematic variables. For example, a data set was constructed (from 30 feedings with simultaneous films and electromyograms) of seven kinematic variables, nine variables derived from measurements of muscle onset and offset times, and 13 variables derived from analyses of electromyogram amplitude. Three different methods of analyzing EMG data were used. 1) The durations of muscle activity were measured relative to the onset of activity in the depressor mandibulae muscle; this constitutes the "onset-offset data," as the only information derived from the electromyograms is the duration and time of the start and end of electrical activity. 2) For each muscle, the amplitude of EMG spikes in each 5-msec interval during a strike was determined, and a mean spike amplitude was calculated for the 5-msec bins; this constitutes the "amplitude data set"; the information derived from the EMG is related to the amplitude of the spikes and the time to peak amplitude. 3) The mean spike amplitude in each 5-msec interval during the strike was multiplied by the mean number of spikes in that interval according to the procedure of Beach et al. ('82); this constitutes the "spike number times ampli-

tude date set"; the information derived from the electromyograms includes the frequency and amplitude of the spikes.

The 5-msec bin width was chosen as the best length of time for myogram analyses because of the short duration of the feeding event (and the nessessity of having at least ten bins per feeding for statistical analysis), and the finding that 5-msec time intervals provided excellent sample sizes for number of spikes and spike amplitudes. In experimental preparations in which low-frequency spikes dominate myograms and in which very slow movements are being studied, longer bin widths may be adequate.

The ability of each of these three methods to provide information about kinematic variation was assessed by multiple regression analysis. Kinematic variables were measured from simultaneously recorded high-speed films and used as dependent variables (one at a time). Variables derived from each of the three types of EMG data sets were used as independent variables to be entered into a multiple regression model. Each model contained EMG variables from a single data set, and thus three models (one for each data set) were constructed for each kinematic variable. To determine which method of EMG analysis provided the most information about the movement pattern, it was necessary only to compare the proportion of variance in any particular kinematic variable explained by the EMG data sets.

It is important to emphasize that all multiple regression models were defined a priori and that variables were entered into the models on the basis of functional morphological criteria and not randomly. For example, when the dependent variable was "peak hyoid depression," the first variables entered into the model were the activity patterns of the hyoid muscles. As a preliminary aid in interpreting the relationships among the variables, we present correlation matrices for a portion of two of the smaller data sets (Tables 1 and 2).

RESULTS

Morphology

General

Some descriptions of head morphology in ambystomatid salamanders are available (e.g., Carroll and Holmes, '80; Eaton, '36; Edgeworth, '35; Jarvik, '63; Keller, '46; Krogh and Tanner, '72; Larson and Guthrie, '75; Luther, '14; Piatt, '38, '39, '40; Severtzov, '68; Valentine and Dennis, '64), but these descriptions do not provide a complete description of larval skull osteology and myology in a functional context. To provide a basis for the experimental data and functional analysis presented here, a description is provided of key osteological and myological features of the head in larval *Ambystoma mexicanum*, with comparative references to *A. tigrinum*, *A. ordinarium*, and *A. dumerilii*. Particular attention is paid to those muscles and aspects of cranial morphology that are relevant to the functional analysis.

As an aid to interpreting the morphology of the head and the movement and muscle activity patterns discussed later, schematic lateral and ventral views of the head of *Ambystoma mexicanum* are presented in Figure 1.

Abbreviations

AME,	Adductor mandibulae externus muscle
AMI	Adductor mandibulae internus muscle
AT,	Atlas vertebra
AX,	Axis vertebra
BH,	Branchiohyoideus muscle
BHY,	Basihyal cartilage
CB,	Ceratobranchial cartilage
CB1, 4,	Ceratobranchial cartilages one and four
CH,	Ceratohyal cartilage
CM,	Coracomandibularis muscle
D	Dentary bone
DM,	Depressor mandibulae muscle
EP,	Epaxial muscles
FR,	Frontal bone
GB,	Gill bars
GF,	Gill filaments
GR,	Gill rakers
H,	Humerus
HB,	Hypobranchial cartilage
HH,	Hypohyal cartilage
HY,	Hypaxial muscles
IH,	Interhyoideus muscle
IMA,	Intermandibularis anterior muscle
IMP,	Intermandibularis posterior muscle
LB,	Levatores branchiarum muscles
MHL,	Mandibulohyoid ligament
MX,	Maxillary bone
NA,	Neural arch
NS,	Neural spine
OD,	Odontoid process on atlas vertebra
OT,	Fused opisthotic and exoccipital
PA,	Parietal bone
PC,	Procoracoid cartilage
PE,	Pectoralis muscle
PMX,	Premaxillary bone
PT,	Pterygoid bone
Q,	Quadrate bone
R,	Rib
RC,	Rectus cervicis muscle
S,	Scapula
SC,	Scapular cartilage
SCO,	Supracoracoideus muscle
SQ,	Squamosal bone
TV,	Transverse process on vertebra

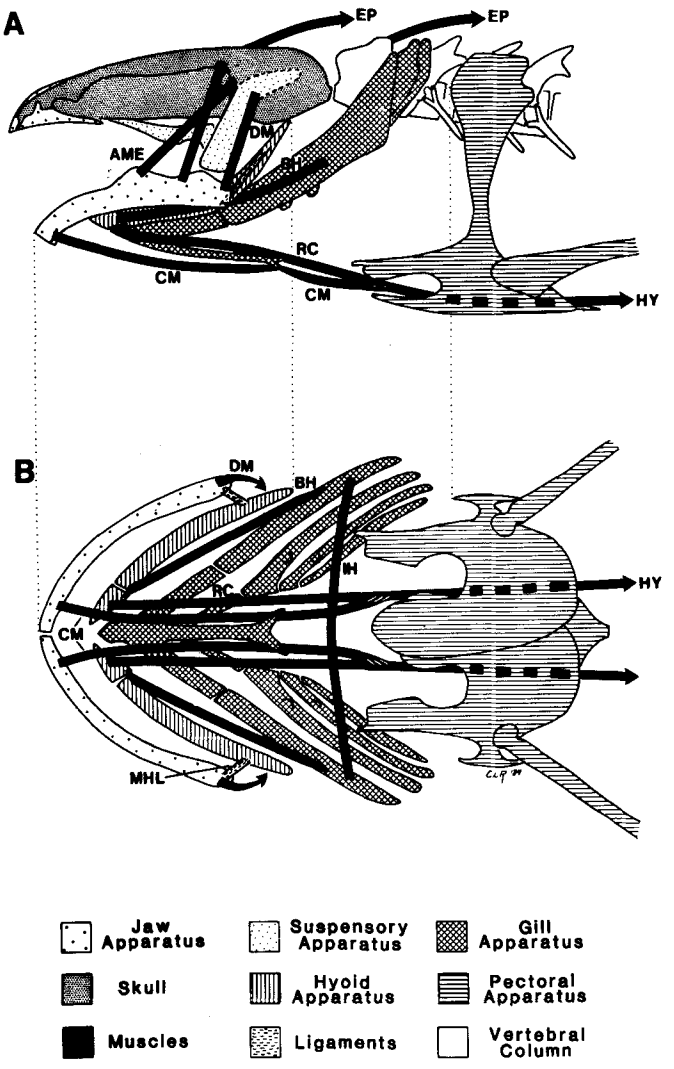

Fig. 1. A, B. Schematic diagram of the major functional components in the head of *Ambystoma mexicanum*. Note the presence of a mandibulohyoid ligament (MHL) that connects the ceratohyal cartilage with the mandible. See the list of abbreviations for this and subsequent figures.

Osteology

The major functional units of the head are the skull, lower jaw, hyoid apparatus, pectoral apparatus, vertebral column, and branchial apparatus (Fig. 1). Relatively little movement occurs between bones within the skull although the premaxillae and maxillae are not rigidly attached to adjacent bones (Figs. 2–4, PMX, MX). All four species studied have teeth on four bones: the premaxilla, maxilla, vomer, and pterygoid.

The suspensorium has only limited mediolateral mobility, and the range of movement is not sufficient to produce major changes in the volume of the buccal cavity. The small degree of suspensorial mobility that is present is due to the relatively flexible attachment of the squamosal to the skull in the form of a flat, broad articulation with the otic and parietal regions (Figs. 2, 3, SQ).

The articulation of the skull with the vertebral column exhibits some variation between species. *Ambystoma dumerilii* displays

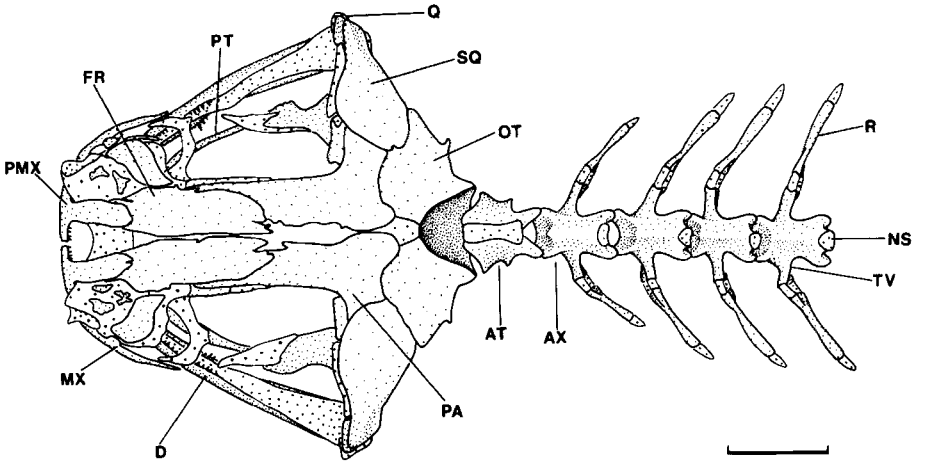

Fig. 2. Dorsal view of the skull and anterior vertebrae of *Ambystoma mexicanum*. Bar = 0.5 cm.

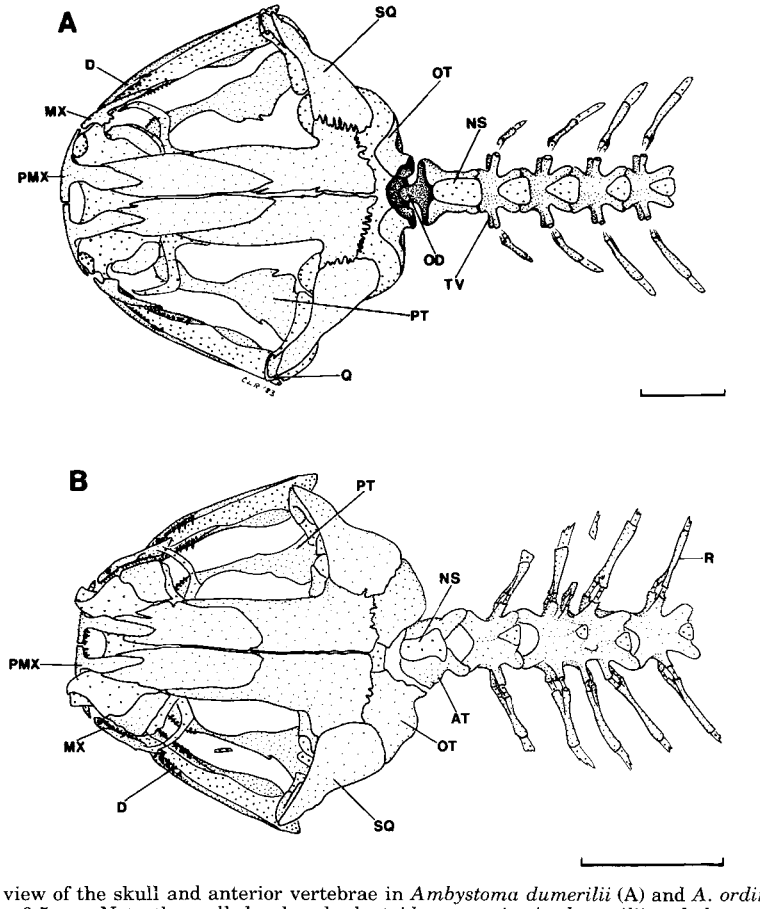

Fig. 3. Dorsal view of the skull and anterior vertebrae in *Ambystoma dumerilii* (A) and *A. ordinarium* (B). Bar for both panels = 0.5 cm. Note the well developed odontoid process in *A. dumerilii* and the asymmetry of the craniovertebral articulation in *A. ordinarium*.

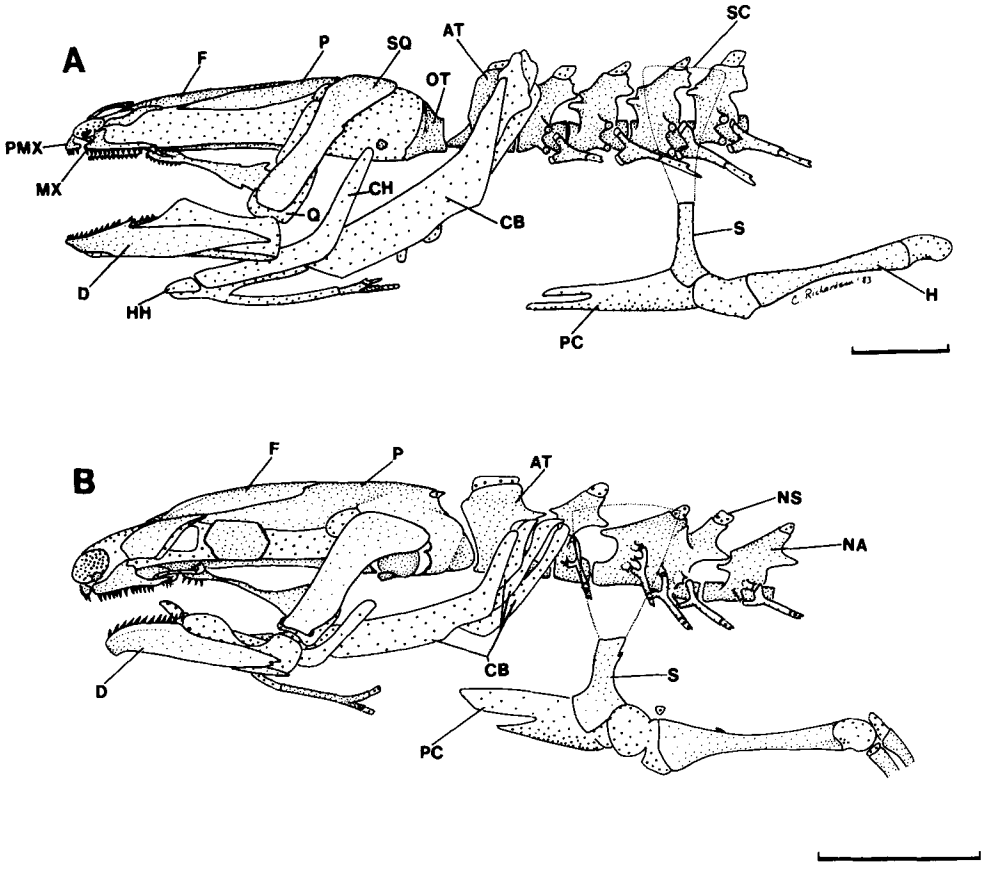

Fig. 4. Lateral views of the skull, anterior vertebrae, and the pectoral girdle in *Ambystoma dumerilii* (A) and *A. ordinarium* (B). In A the hyoid apparatus is shown depressed below the mandible; in B, the hyoid is illustrated in its protracted position. Note the differing articulations between the atlas vertebra and the skull in the two species. Bars = 0.5 cm.

the largest gap between the back of the skull and the first (atlas) vertebra (Figs. 3A, 4A), and the odontoid process of the atlas is better developed than in *A. mexicanum* and *ordinarium*. *A. dumerilii* thus possesses the greatest possible range of cranial elevation. *A. ordinarium* (Fig. 4B) has a relatively small space between the atlas and the skull, and a more elongate neural arch and spine. Some left-right asymmetries in the craniovertebral articulations were found (Fig. 3B). All four species studied possess an odontoid process on the atlas that abuts the parasphenoid and exoccipitals.

The hyoid apparatus is composed of paired ceratohyals that articulate ventrally with smaller hypohyal cartilages (Figs. 4, 5). The ceratohyal has a prominent posterodorsal extension from which arises the mandibulohyoid ligament (Fig. 1, MHL; Figs. 4, 5, CH, HH). This ligament attaches to the posteroventral aspect of the mandible. Depression of the anterior tip of the hyoid ventrally results in a posterodorsal movement of the ceratohyal that causes the mandible to rotate ventrally because of tension in the mandibulohyoid ligament.

Posterior to the hyoid apparatus, the hypobranchial cartilages abut the median basibranchial cartilages and form the floor of the gill (branchial) apparatus (Fig. 5, CB). The larger ceratobranchials curve posterodorsally to reach the level of the vertebral bodies or beyond (Fig. 4, CB). A significant feature of the morphology of the branchial apparatus from a functional perspective is the presence of gill rakers on the ceratobranchials (Fig. 6). The gill rakers on adjacent ceratobranchials are staggered in position and interlock when the gill bars are opposed

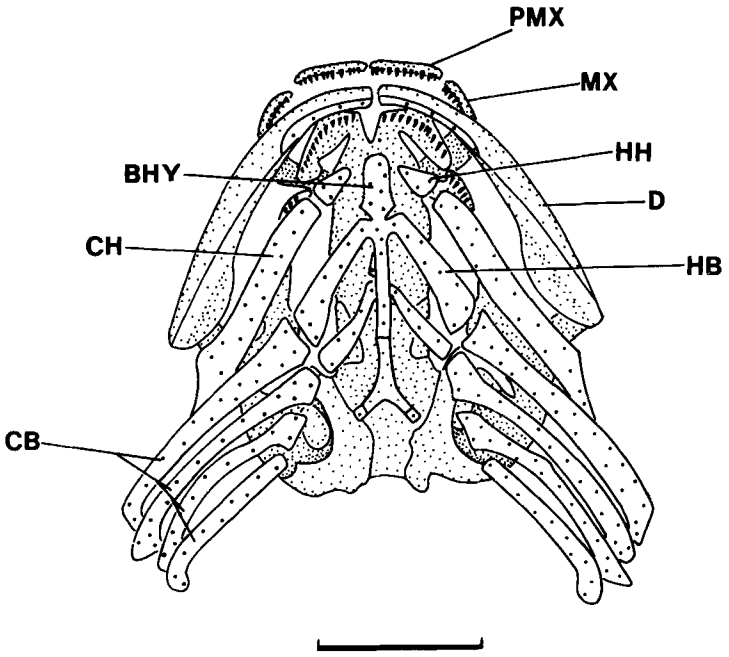

Fig. 5. Ventral view of the branchial and hyoid regions in *Ambystoma ordinarium*. The premaxillary, maxillary, vomerine, and pterygoid teeth are visible on the skull. Bar = 0.5 cm.

to each other. The interlocking is precise, and an effective seal is formed at the back of the head when the gill bars are adducted.

Myology

The most prominent dorsal muscles are the large epaxial muscle bundles that insert broadly on the back of the skull (Figs. 7, 8, EP). The levatores branchiarum (Fig. 8, LB) take their origin mainly from the surface of the epaxial muscles. *A. dumerilii*, in contrast to the other species, possesses a specialized bundle of deep, medial epaxialis fibers that insert via a separate tendon on the first neural spine (Figs. 3, 4, NS). Separate bundles of epaxial muscle fibers also arise from this tendon and from the first neural spine to insert on the posterodorsal region of the skull.

The two major adductors of the lower jaw are the adductor mandibulae internus and externus. The internal adductor has a broad origin from the otic, parietal, and pterygoid regions of the skull (Figs. 7, 8, AMI). In *A. dumerilii*, the most posterodorsal fibers of the internal adductor separate into a distinct bundle that originates via a short tendon from the first neural spine. Because these fibers pass dorsal to the craniovertebral articulation, contraction of the adductor mandibulae internus will raise the skull on the vertebral column. Thus in A. *dumerilii* both the epaxialis and adductor mandibulae internus must be considered as mediating cranial elevation. As shown on the right side of the specimen illustrated in Figure 8, there is a slight separation of deep internal adductor fibers originating posterior to the eye from the overlying main bulk of the adductor internus. The insertion of the internal adductor is onto the medial and dorsal surface of the mandible. The most medial portion of the tendon of the adductor mandibulae externus joins the internal adductor tendon just before its insertion. The origin of the external adductor is in the cartilaginous auditory bulla and in the squamosal (Figs. 7, 8, AME).

The depressor mandibulae (Figs. 7–9, DM) has an extensive origin from the posterolateral wall of the skull (including the opisthotic) and extends medially ventral to the levatores branchiarum and the epaxial muscles. In addition, a small bundle of fibers from the branchiohyoideus joins the ventral edge of the depressor mandibulae (Fig. 7, BH). There are two relatively distinct portions of

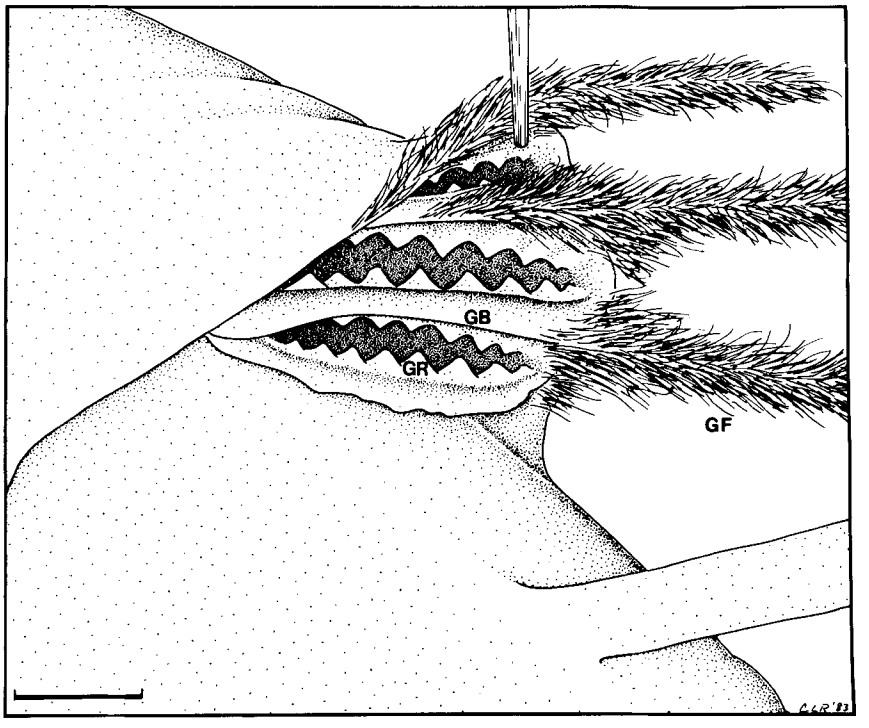

Fig. 6. Ventral view of the branchial region in *Ambystoma mexicanum*. The side of the head has been pulled laterally by the forceps shown at the top to expose the gill bars (ceratobranchials) and the gill rakers. Note the interlocking gill rakers on opposing gill bars. When adjacent gill bars are adducted, the gill rakers interdigitate to form a high resistance to water flow. Bar = 0.5 cm.

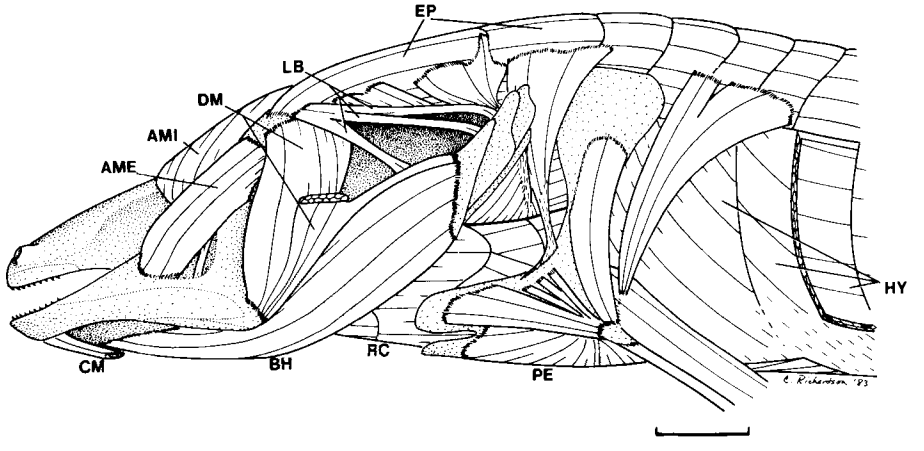

Fig. 7. Lateral view of the cranial musculature of *Ambystoma dumerilii*. The coracomandibularis (CM) has been cut posterior to its origin at the mandibular symphysis. The depressor mandibulae muscle (DM) has two heads, one of which has been cut to illustrate the origin of the medial head and the levatores branchiarum (LB). Bar = 0.5 cm.

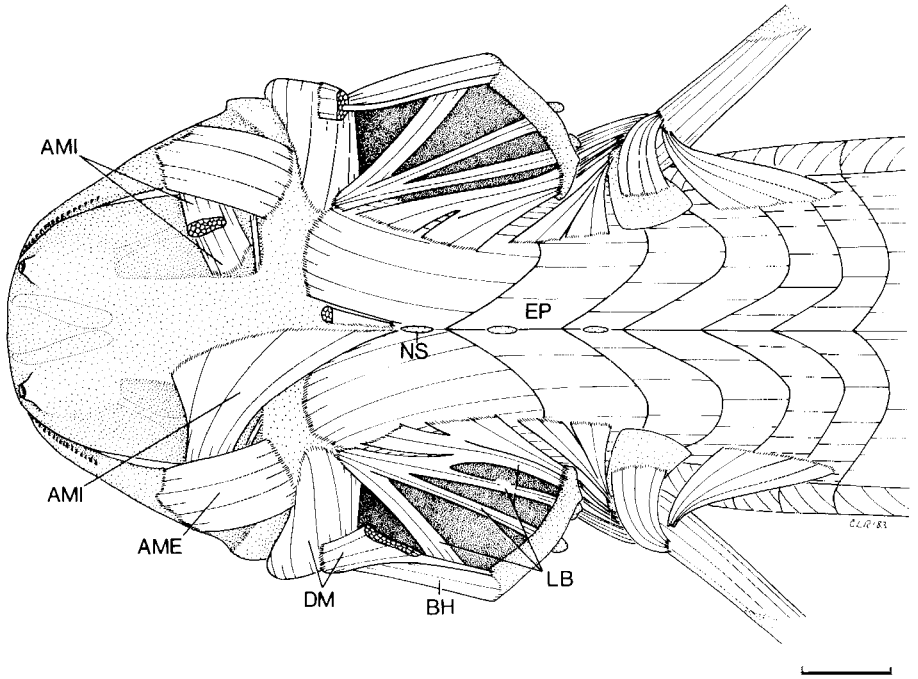

Fig. 8. Dorsal view of the cranial musculature of *Ambystoma dumerilii*. The adductor musculature is shown in its natural condition on the left side (and the posterodorsal fibers of the adductor mandibulae internus, AMI, can be seen extending toward the first neural spine). On the right side, the superficial fibers of the internal adductor have been cut to show the origin of the deep fibers. The origin of the superficial adductor fibers on the right side is shown anterior to the neural spine. Bar = 0.5 cm.

the depressor mandibulae, a thinner superficial division and a more massive medial division. The depressor mandibulae inserts via a short tendon onto the angle of the mandible.

The branchiohyoideus originates only from the first ceratobranchial and inserts along the ceratohyal (Figs. 7, 9, BH). The medial fibers of the branchiohyoideus insert on the hypohyal. This muscle has a complex line of action that spans several joints. Based on the activity pattern reported below, the branchiohyoideus probably mediates hyoid retraction and possibly also produces ceratobranchial abduction in the absence of antagonistic activity.

The coracomandibularis originates near the mandibular symphysis just dorsal and lateral to the intermandibularis anterior (Fig. 9, CM). This muscle passes posteriorly to insert on the "urohyal" and then continues from this point posteriorly to form a relatively distinct muscle bundle apposed ventrally to the rectus cervicis (Fig. 9, RC). Fibers continuous with those of the coracomandibularis can be traced dorsal to the pectoral girdle, where they become indistinguishable from the rectus cervicis. The coracomandibularis mediates both mandibular abduction and hyoid protraction. If the position of the mandible is fixed by the action of the internal and/or external adductor muscles, then contraction of the coracomandibularis will compress the buccal cavity and protract the hyoid.

The rectus cervicis (= sternohyoideus) has a distinct insertion along the basibranchial cartilage, and some fibers also attach to hypobranchial 1 and the basihyal. The rectus cervicis continues posteriorly dorsal to the pectoral girdle, which has a loose fibrous attachment to the underlying musculature and a more well defined attachment to a small piece of cartilage imbedded in the superficial rectus cervicis fibers. Posterior to the shoulder girdle, fibers of the rectus cervicis continue (across myosepta) as the rectus abdominus. Some shoulder muscles take their origin from rectus cervicis (e.g., Fig. 9, PE). The rectus cervicis is the major muscle that mediates posteroventral depression and retraction of the hyoid (and perforce the

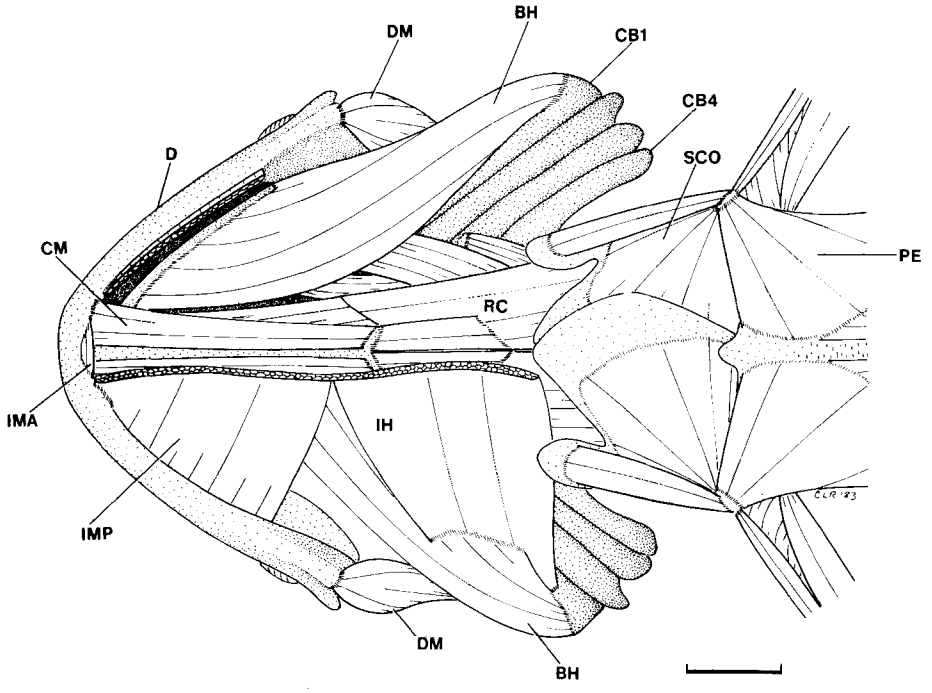

Fig. 9. Ventral view of the cranial muscles of *Ambystoma dumerilii*. The intermandibularis posterior and interhyoideus (IMP and IH) have been removed on the left side to show the course of the deeper musculature. On the right side, the anterior fibers of the interhyoideus have been removed to illustrate the relationship of the branchiohyoideus (BH) to the mandible and depressor mandibulae (DM). Bar = 0.5 cm.

branchial apparatus). Contraction of the rectus cervicis moves the basihyal posteriorly and ventrally and places the mandibulohyoid ligament in tension.

The hypaxial musculature is a complex assemblage of muscle fiber layers that become difficult to separate near their cranial aspect. In general, the hypaxial musculature covers the body wall ventrolaterally and is distinct from the rectus cervicis and its posterior extensions along the midline of the body ventrally. There is a superficial hypaxial fiber layer that runs anterodorsally, and this is traditionally called the external oblique (Fig. 7). At this level, the deeper fibers are oriented longitudinally, as shown in the cut section of the hypaxialis (Fig. 7, HY). Deep to the external oblique fibers at the level of the scapula, internal oblique fibers run anteroventrally to merge with fibers of the rectus cervicis.

The intermandibularis posterior is a well developed muscle that spans the mandibular rami (Fig. 9, IMP). The muscle mass is thickest laterally and thins to a connective tissue sheet with relatively few muscle fibers toward the midline. This muscle lies ventral to the coracomandibularis and rectus cervicis and acts to elevate the depressed hyoid apparatus and compress the buccal cavity dorsoventrally.

Posterior to the intermandibularis posterior, the interhyoideus muscle originates from the surface of the branchiohyoideus and the upper limb and angle of the ceratohyal (Fig. 9, IH). The muscle fibers extend transversely toward the midline and form the posterior portion of the branchial membrane that covers the throat ventrally. The fibers of the interhyoideus on each side meet in the midline and pass dorsal to the posterior fibers of the intermandibularis posterior to form a complete muscular sheath ventral to the hyoid and branchial apparati. Some authors (e.g., Walker, '75, p. 127) refer to the posterior fibers of the interhyoideus as the "sphincter colli" (= constrictor colli); others refer to these fibers as the "interhyoideus posterior" (e.g., Piatt, '40; Jarvik, '63). The interhyoideus muscle acts to elevate the depressed hyoid apparatus and to adduct the ceratobranchials.

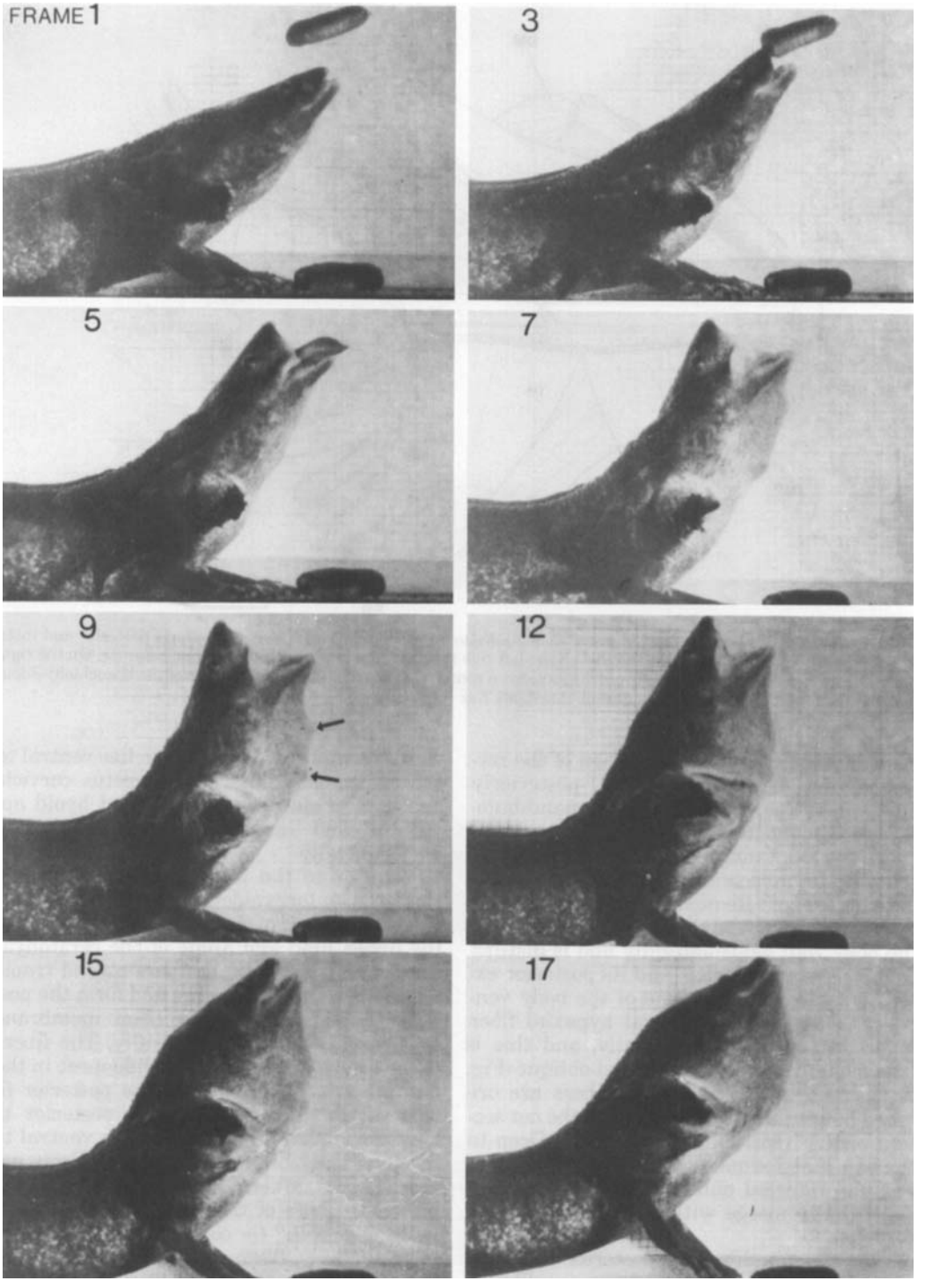

Fig. 10. Eight frames from a film (taken at 200 frames per sec) of prey capture in *Ambystoma dumerilii*. The number of each frame within the sequence is indicated in the upper left corner of each image. The entire sequence lasts 85 msec. Arrows in frame 9 indicate the prominences caused in the throat region by the depressed hyoid. Note the extensive head lifting and the delay in hyoid depression relative to maximum gape. Abduction of the gill bars begins about frame 9, and spaces between the bars are visible in the last frames.

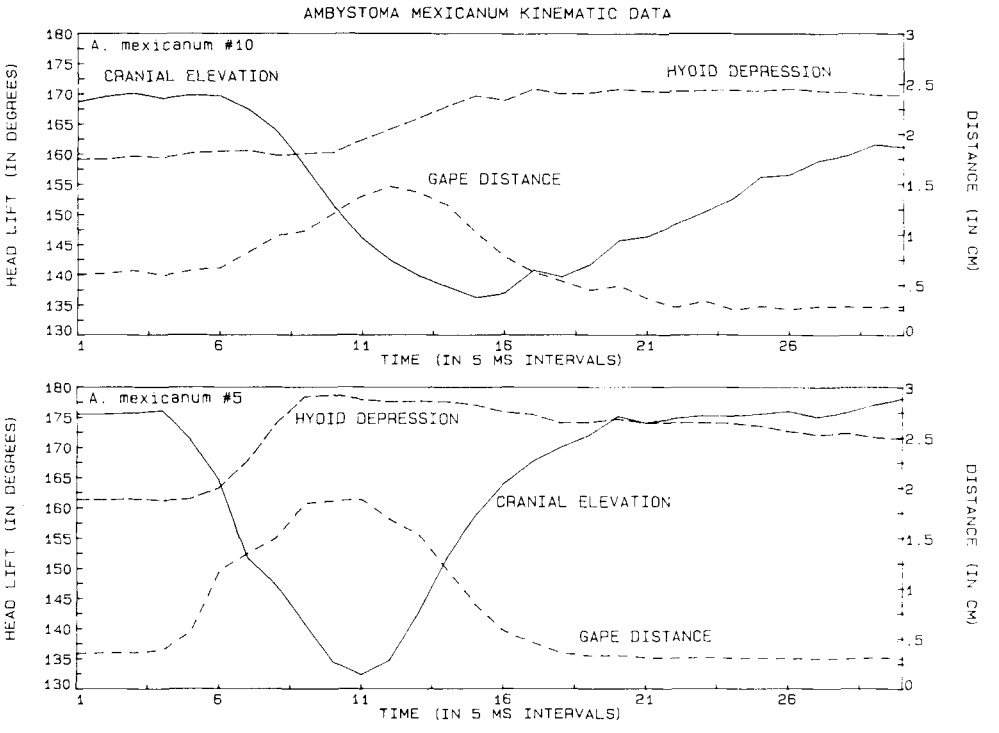

Fig. 11. Graphic representation of the kinematic pattern at the strike in two individual *Ambystoma mexicanum*. Three variables are shown: cranial elevation (solid line, left scale); hyoid depression (large dashes, right scale); and gape distance (short dashes, right scale). Note that cranial elevation is measured as the angle between the body and the head, and thus smaller angles represent greater lifting of the head. These two sequences were chosen to illustrate the extent of variation between feedings and individuals. Note that in *A. mexicanum* number 5 hyoid depression reaches its maximum before peak gape, whereas the reverse is true of individual number 10.

Kinematic and electromyographic patterns

Figure 10 shows a typical pattern of head movement in *A. dumerilii* during a strike at a piece of worm. The entire strike is completed in 85 msec. The increase in gape achieved both by cranial elevation and by depression of the mandible, and the extent of hyoid depression is clearly evident at maximum gape (Fig. 10, arrows in frame 9). As the mouth closes, water begins to flow out between the gill bars, and abduction of the branchial basket is manifested externally by the openings between the gill bars visible below the gills (Fig. 10, frames 12, 15,–17).

Kinematic patterns for three variables in two individual *A. mexicanum* are illustrated in Figure 11, and this figure also provides an indication of the extent of variation in head movements during feeding. Maximum gape usually precedes both peak cranial elevation and peak hyoid depression as in the curves shown for *A. mexicanum* individual number 10 (Fig. 11, upper panel). Occasionally, as shown in the lower panel of Figure 11, maximum cranial elevation and hyoid depression occur synchronously or slightly before peak gape, although this is rare. Mean values for maximum gape and hyoid depression in relation to pressure in the buccal cavity and movements of the gill bars are shown for *A. mexicanum* in Figure 12. Peak hyoid depression occurs significantly later than peak gape (12 msec later), and maximum cranial elevation occurs 15 msec later on average than peak gape.

Electromyographic data obtained from cranial muscles during feeding (Figs. 13, 14) demonstrate that nearly all muscles become active within a very short time and with little variation. The mean time of onset of activity for the nine muscles shown in Figure 14 relative to the start of activity in the depressor mandibulae muscle is −0.34 msec (standard deviation 1.22 msec, N = 208).

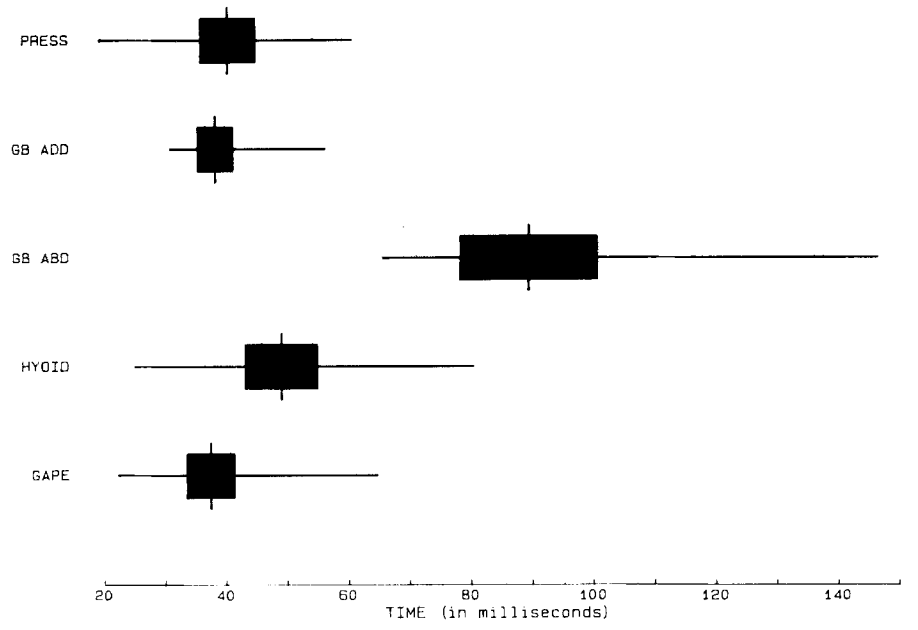

Fig. 12. Bar diagram to illustrate the relative timing of five aspects of the strike in *Ambystoma mexicanum*: PRESS, the time to maximum negative buccal cavity pressure; GB ADD, the time to maximum adduction of the gill bars (ceratobranchials); GB ABD, the time to maximum abduction of the gill bars; HYOID, the time to peak hyoid depression; and GAPE, the time to peak gape. The vertical line for each variable indicates the mean value, the black bars +/− 2 standard errors of the mean, and the horizontal line the range of each variable. The time to peak gape, maximum negative pressure, and maximum gill bar adduction are not significantly different from each other (based on N = 20 feedings).

Thus all muscles recorded are activated nearly simultaneously. The two adductor muscles (Fig. 14, AMI, AME) are active for significantly longer periods than most other muscles (e.g., the depressor mandibulae, rectus cervicis, epaxialis, hypaxialis, and branchiohyoideus, all of which have very similar activity durations). Only two muscles show a double burst pattern at the strike: the intermandibularis posterior and the coracomandibularis. In both these cases, the first burst is similar in duration to the other (nonadductor) muscles (Fig. 14) and occurs during mouth opening; the second burst begins later, near the time when the adductor muscles are ending activity and the mouth has closed. The interhyoideus muscle is active throughout the strike (Fig. 14, IH), although this muscle shows some tendency (albeit a nonsignificant one) to display two bursts in a similar pattern to the intermandibularis posterior.

Figure 15 illustrates the patterns of change in the amplitude of muscle activity during a strike for five muscles in relation to bone movement for the same strikes. The figure shows the average kinematic pattern and the average pattern of spike number times spike amplitude for five muscles in 15 feedings by one individual *A. mexicanum*. On average, muscle activity in the depressor mandibulae begins 15 msec prior to the start of mouth opening. The depressor mandibulae and epaxialis (Fig. 15, DM, EP) show the most rapid increase in amplitude reaching a maximum value within 35 msec. The rectus cervicis and adductor mandibulae externus also reach their peak amplitude at 35 msec, and the internal adductor achieves maximum amplitude at 50 msec. Comparison of the traces for the depressor mandibulae and internal adductor in Figure 15 clearly illustrates that there are different levels of muscle activity during mouth opening, which are masked by consideration of onset and offset times alone.

The coefficients of variation for both the kinematic and spike amplitude analysis in Figure 15 shows that the least variation in both kinematics and muscle activity occurs

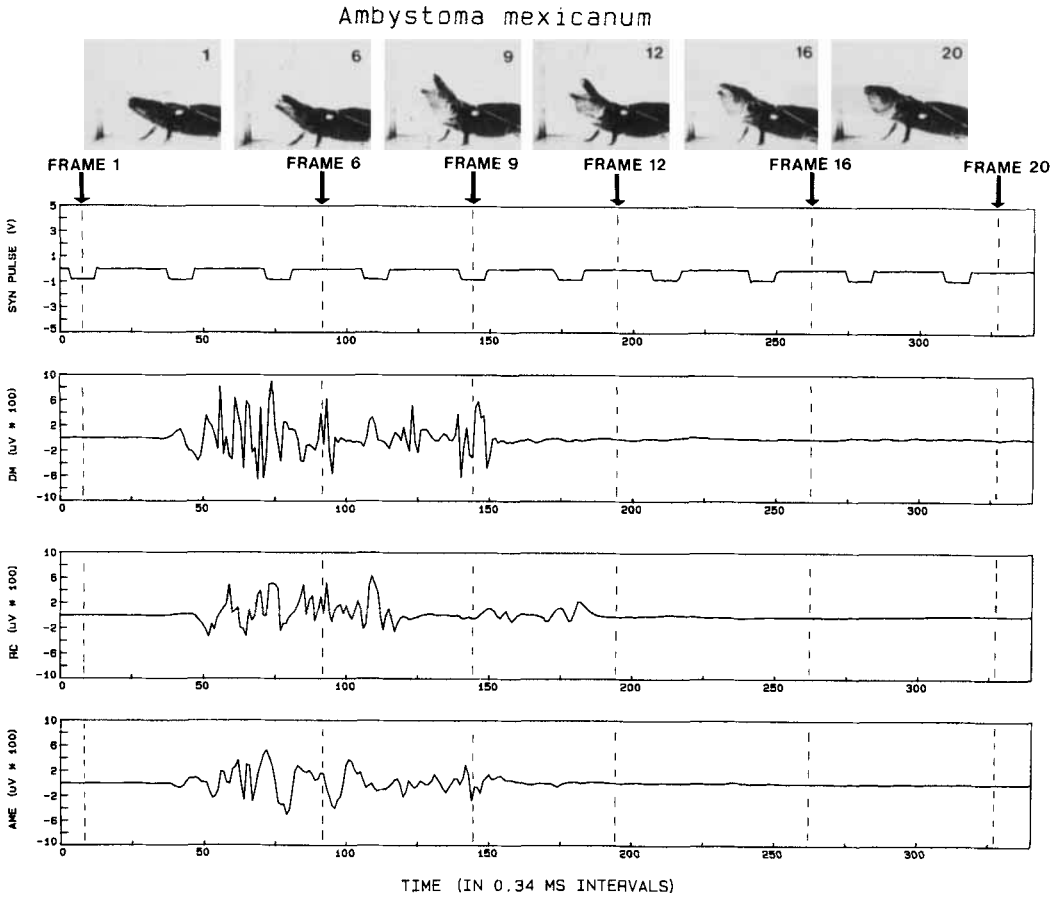

Fig. 13. Representative data from experiments in which films taken at 200 frames per sec were synchronized with EMG recordings from five cranial muscles. Three muscles are illustrated, the depressor mandibulae (DM), rectus cervicis (RC), and the external adductor mandibulae (AME), and the synchronization pulse (SYN) is shown for reference. Vertical dashed lines indicate the correlation of each film frame at the top with the EMG record.

during a 10–20-msec period after the mouth has started to open. The coefficients of variation for all parameters reach a minimum at a mean time of 11.9 msec after the mouth starts to open (standard deviation 8.8 msec). This pattern is not due simply to synchrony in maximum amplitude of activity as the minimum coefficients do not always occur with maximum activity; the standard errors of the mean amplitudes also are least when the coefficients of variation reach their minimum. The internal adductor muscle contributes the most to the variation in these coefficients as it reaches its minimum 30 msec after the mouth starts to open. With this exception, the other muscles and the head movements display considerable concordance in the time of least variation, and this time occurs about 10 msec after the mouth starts to open.

The Pearson product-moment correlations among the simultaneously recorded kinematic and electromyographic variables are generally low (Table 1), with only two of 66 possible values being greater than 0.5. The mean correlation for all variables shown in Table 1 is 0.10 (standard deviation 0.23). The pair of variables with the highest correlation (0.87) is the DM-RC (difference in onset time of activity in the rectus cervicis and depressor mandibulae) and the DM-AMI (difference in onset of the internal adductor and the depressor mandibulae).

Table 2 presents the results of the comparison between three analytical methods

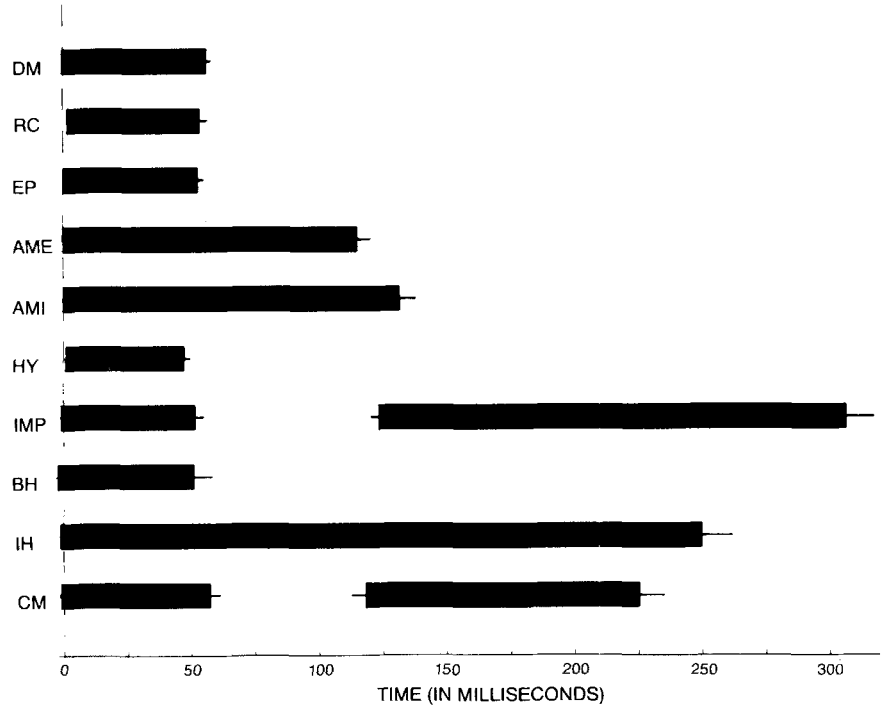

Fig. 14. Summary bar diagram to illustrate the pattern of onset and offset of activity in 10 cranial muscles in *Ambystoma mexicanum*. The figure summarizes data from 216 feedings, although not all muscles were recorded in every experiment. Muscle onsets were measured relative to the start of activity in the depressor mandibulae (DM). Only two muscles have a double burst activity pattern: the intermandibularis posterior (IMP) and the coracomandibularis (CM). All muscles begin activity within 0.34 msec of each other.

TABLE 1. Correlation matrix for selected kinematic and electromyographic variables (simultaneously recorded) in one individual Ambystoma mexicanum (No. 10)[1]

	(1)	(2)	(3)	(4)	(5)	(6)	(7)	(8)	(9)	(10)	(11)	(12)
(1) Peak head angle (°)	1	.54**	.16	.42*	.02	.04	.02	.36*	−.10	−.12	−.08	−.18
(2) Peak hyoid depression (cm)		1	.28	.30	.04	.18	.06	.42*	−.10	−.02	.10	.10
(3) Peak gape distance (cm)			1	.30	−.13	.00	.24	.11	.11	.03	−.13	.12
(4) Time to peak gape (msec)				1	.48*	−.01	.02	.26	.24	.10	.04	.06
(5) Time to peak hyoid depression (cm)					1	−.14	−.15	.37*	.08	−.06	.22	.23
(6) DM (msec)						1	−.15	.46*	.25	.21	−.36*	.47*
(7) RC (msec)							1	−.05	−.40*	−.18	.40*	−.22
(8) AMI (msec)								1	.04	−.09	−.20	.21
(9) DM-RC (msec)									1	.87**	−.17	.42*
(10) DM-AMI (msec)										1	.00	.29
(11) RC spike no. times amplitude											1	−.13
(12) AMI spike no. times amplitude												1

[1]See Materials and Methods for a description of the variables. Correlations (r) are based on a sample size of N = 29.
*Significant at the 0.05 level.
**Significant at the 0.01 level.

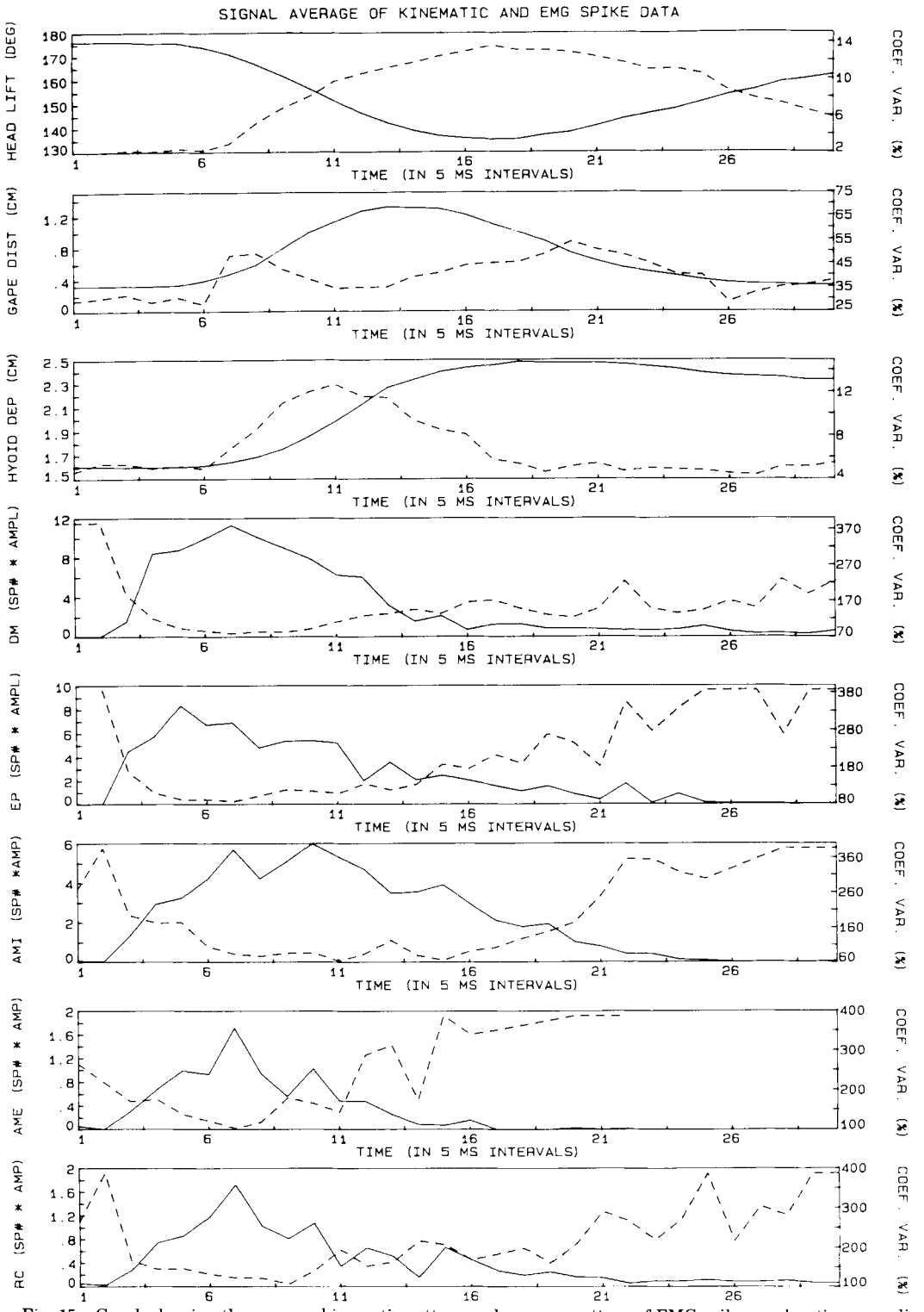

Fig. 15. Graph showing the average kinematic pattern and average pattern of EMG spike number times amplitude for 15 feedings by *Ambystoma mexicanum*. For each of the 15 feedings, the skull movements and myograms were obtained simultaneously. Spike number times amplitude values (solid lines) were calculated using 5-msec bins (see text), and these analyses were synchronized with kinematic measurements taken at 5-msec intervals. The left scales indicate the units of measurement; the right scale indicates the coefficients of variation (dashed lines) for the mean values plotted. Gape cycle times for these feedings ranged between 80 and 110 msec. Note that the coefficients of variation tend to be least as the mouth begins to open, at the 30-msec time interval on the x-axis. Note the units for the myograms shown are the product of spike number (a dimensionless parameter) and spike amplitude (in volts). See text for further discussion.

TABLE 2. Comparison of three analytical approaches to the information content of electromyograms[1]

Model type	Dependent variables (1) Peak head angle (°)	(2) Peak hyoid depression (cm)	(3) Peak gape (cm)	(4) Time to peak gape (msec)	(5) Time to peak hyoid depression (msec)	(6) Time of gape cycle (msec)	(7) Time to peak head lift (msec)
Onset and offset EMG variables	.21 (17)	.25 (17)	.30 (17)	.34 (17)	.32 (17)	.23 (17)	.22 (17)
Spike no. times amplitude EMG variables	.72 (18)	.31 (18)	.41 (18)	.29 (18)	.22 (18)	.56 (18)	.24 (18)
Spike amplitude EMG variables	.69 (18)	.18 (18)	.31 (18)	.21 (18)	.14 (18)	.49 (18)	.24 (18)

[1]Values in each cell are the R^2 (degrees of freedom) of a multiple regression model predicting each of the seven dependent variables. The models differ for each dependent variable as models were constructed based on functional morphological criteria (see text for discussion).

for obtaining information from electromyograms. The "spike number times amplitude method" produced a higher R^2 value than the "spike amplitude method" in every case but one (variable 7), in which the R^2 values were equal. This difference is significant at the 0.01 level (Wilcoxon signed-ranks test). There is no consistent difference in the variance explained by the "spike amplitude method" and the "onset-offset method." For the seven possible comparisons, the onset-offset analysis produced a higher R^2 value three times. In general, the "spike number times amplitude" method is a more powerful predictor of kinematic variation than the "onset-offset" method, although the difference in performance is significant only at the 0.15 level. However, the "onset-offset" method generates a higher R^2 in only two of seven cases (Table 2), and in both these the difference is relatively slight.

Buccal pressure and gill impedance patterns

Figure 16 illustrates the pattern of pressure change in the buccal cavity of *A. mexicanum* in relation to muscle activity in four muscles and gape distance (transduced with impedance electrodes). Similar data are also shown to indicate the sequence of gill bar movements (adduction as the buccal pressure drops, then abduction) in relation to muscle activity patterns (Fig. 16B). Peak adduction of the gill bars occurs synchronously with maximum gape and maximum negative buccal pressure (i.e., there is no significant difference among the three variables; Fig. 12). Maximum abduction of the gill bars occurs at a mean time of 89.5 msec, significantly later than peak gape or peak negative pressure. Maximum negative pressures in the buccal cavity reached −25 mm Hg; the mean was 12 mmHg.

The Pearson product-moment correlations among (simultaneously recorded) EMG, pressure, and impedance variables are given in Table 3. The correlations are higher on average than those among kinematic and EMG variables (Table 1), with 12 of 45 possible correlations greater than 0.50. Noteworthy correlations include those between gill bar adduction and pressure variables (Table 3, variables 7–9), between the time to peak pressure and activity duration in the depressor mandibulae and epaxialis (Table 3, variables 1, 4, and 8), and between the integrated buccal pressure and rectus cervicis activity (variables 2 and 9).

An analysis of the ability of EMG variables to predict variation in simultaneously recorded pressure patterns (from which four variables were derived) is shown in Table 4. Four different multiple regression models were constructed with differing functional components. The striking result is that the duration of activity in the rectus cervicis muscle is the only variable with a significant coefficient in predicting the maximum negative buccal pressure and the integrated buccal pressure for the full model (Table 4, model D). The difference in onset time of the depressor mandibulae and internal adductor was significant (for the full model) in predicting the time duration of negative buccal pressure (Table 4, dependent variable 2).

Similar analyses using the magnitude of gill bar adduction as a dependent variable show that the DM-RC and DM-AMI variables have significant negative coefficients.

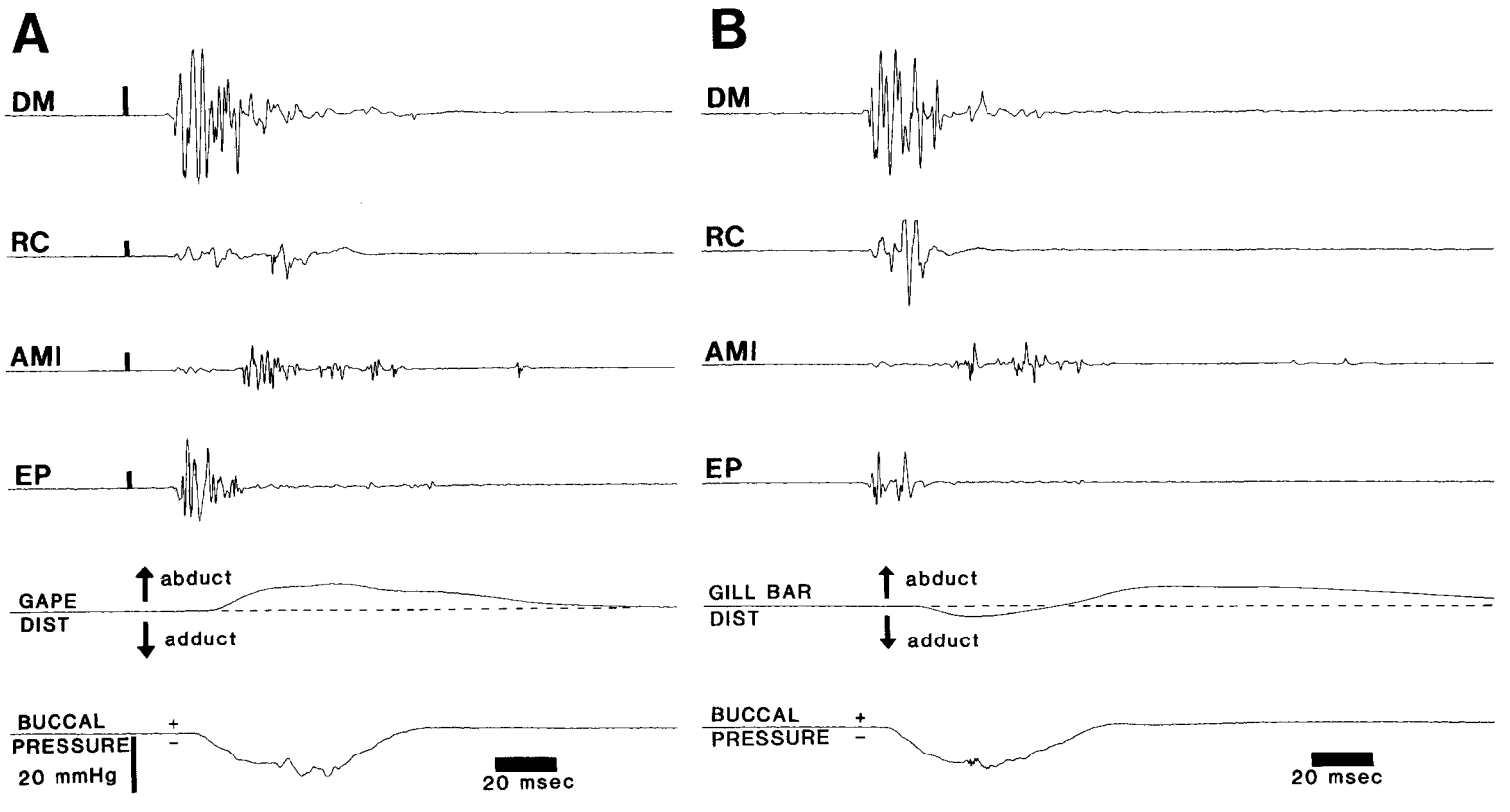

Fig. 16. Representative data from an experiment in which myograms were obtained simultaneously with measurements of pressure in the buccal cavity and in which gape distance (A) and gill bar distance (B) were transduced using an impedance converter. Note the relationship between maximum negative pressure in the buccal cavity, peak gape, and adduction of the gill bars. The measurements of gill bar distance clearly show that the ceratobranchials are *adducted* as the mouth opens and that the branchial apparatus functions as a resistance to water influx from behind the head as the mouth opens. The resistance then decreases as the branchial basket abducts, and water flows through the buccal cavity and exits posteriorly.

TABLE 3. Correlation matrix for selected electromyographic, pressure, and impedance variables (simultaneously recorded) in one individual Ambystoma mexicanum (No. 10)[1]

	(1)	(2)	(3)	(4)	(5)	(6)	(7)	(8)	(9)	(10)
(1) DM (msec)	1	.72**	−.15	.76**	.36	−.51*	.15	.52*	.38	.16
(2) RC (msec)		1	.03	.60**	.06	−.57**	.28	.50**	.62**	.10
(3) AMI (msec)			1	.09	−.09	−.30	−.05	.07	.06	−.21
(4) EP (msec)				1	−.04	−.60**	.40	.68**	.40	.13
(5) DM-RC (msec)					1	−.17	−.61**	−.30	−.16	.10
(6) DM-AMI (msec)						1	−.27	−.30	−.44*	.16
(7) Maximum gill bar adduction							1	.57**	.42	.07
(8) Time to peak buccal pressure (msec)								1	.29	−.22
(9) Integrated buccal pressure ($mmHg^2$)									1	−.16
(10) Time to peak gill bar adduction (msec)										1

[1]See Materials and Methods for a description of the variables. Correlations (r) are based on a sample size of N = 20.
*Significant at the 0.05 level.
**Significant at the 0.01 level.

TABLE 4. Summary of the results of multiple regression analyses in which electromyographic variables are used to predict buccal pressure variables (recorded simultaneously)[1]

	Dependent variables (Y)			
Model[2]	(1) Maximum buccal pressure (mmHg)	(2) Duration of negative buccal pressure (msec)	(3) Time to peak buccal pressure (msec)	(4) Integrated buccal pressure ($mmHg^2$)
A) Nonepaxial model $Y = b_0 + b_1(DM\text{-}RC) + b_2(RC) + b_3(DM) + b_4(DM-AMI)$	.45 (11) —	.42 (11) (DM, DM-AMI)	.54 (11) (DM, DM-RC)	.44 (11) —
B) Epaxial model $Y = b_0 + b_1(RC) + b_2(DM) + b_3(DM\text{-}EP) + b_4(EP)$	.56 (11) (DM, RC, EP)	.14 (11) —	.55 (11) (EP)	.59 (11) (RC, DM-EP)
C) Rectus cervicis model $Y = b_0 + b_1(RC)$	.30 (14) (RC)	.02 (14) —	.25 (14) (RC)	.39 (14) (RC)
D) Full model $Y = b_0 + b_1(DM\text{-}RC) + b_2(RC) + b_3(DM) + b_4(DM\text{-}AMI) + b_5(AMI) + b_6(DM\text{-}EP) + b_7(EP)$	.61 (8) (RC)	.58 (8) —	.64 (8) —	.59 (8) (RC)

[1]Data in the table are R^2 values for the models and, in parenthesis, the degrees of freedom. Beneath each entry are listed the variables (if any) with statistically significant coefficients in the model. See Materials and Methods for a description of the variables.
[2]Variables listed in the order entered into the model; coefficients in the models are indicated by b_0, b_1, etc.

Thus the degree to which the gill bars are adducted during a strike is significantly inversely related to the magnitude of the difference in the onset of electrical activity in the rectus cervicis and internal adductor muscles. We emphasize that these multiple regression models are based on only 8–11 degrees of freedom, which provides relatively little statistical power for hypothesis testing. In this sense, significance tests should be viewed as relatively conservative statements of biological importance.

The patterns of correlation among variables do not contain a component that can be attributed to differences in feeding performance as a result of satiation or other sequential changes during a particular feeding sequence. Figure 17 illustrates the relationship of integrated buccal pressure and the number of prey eaten in a particular repre-

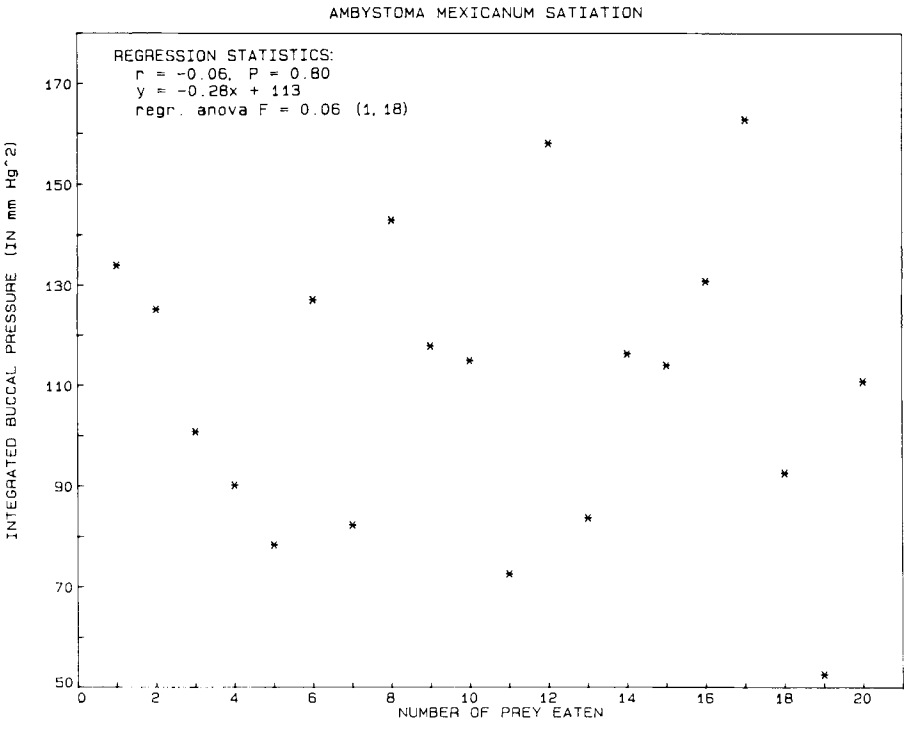

Fig. 17. Graph of the relationship between the integrated buccal pressure (measured as the area under the negative portion of the buccal pressure trace) and the number of prey eaten. The data represent sequential feedings of one individual *Ambystoma mexicanum* in one experiment. The regression statistics shown in the upper left indicate that there is no "satiation effect" in which pressure (or any other variable similarly analyzed) changes systematically with the number of prey consumed during an experiment.

sentative experiment (one sequence of feedings in one individual on 1 day). There is no significant slope to the regression line that might indicate a satiation effect on the variable. Similar results were obtained for other variables analyzed.

DISCUSSION

Over the last 10 years, there have been relatively few quantitative, experimental studies of the functional morphology of feeding in amphibians. Most of the investigations that are available (Bemis et al., '83; Larson and Guthrie, '75; Lombard and Wake, '76, '77; Roth, '76; Thexton et al., '77; and see Wake, '82) have focused on terrestrial feeding and few (Matthes, '34, is an exception) have considered the mechanism of aquatic prey capture in any detail. In this paper we have focused on the mechanism of aquatic prey capture in ambystomatid salamanders with the aims of 1) providing a detailed experimental analysis of the functional morphology of prey capture, 2) comparing the biomechanics of suction feeding in salamanders with previous experimental results and models available for fishes, 3) using the mechanism of prey capture in aquatic ambystomatids as a system in which to test alternative methods of analyzing electromyographic data, and 4) integrating the currently available data on skull structure and function in lower vertebrates with new data provided here and contributing an assessment of patterns of evolution in the lower vertebrate skull. Each of these aims will now be discussed.

Functional morphology

Among the four species of ambystomatid salamanders studied, the kinematic patterns during prey capture are very similar. Individual salamanders often show some variability in the relative timing of head move-

ments between feedings, but the average pattern for all feedings is clear: Peak hyoid depression and cranial elevation occur after maximum gape. For the purpose of describing the process of initial prey capture, it is useful to consider the terminology used for fishes (Lauder, '83c). The *preparatory* phase of the strike is defined as the period of time prior to the start of mouth opening. The *expansive* phase of the strike is defined as the time from the onset of mouth opening to peak gape. The *compressive* phase is the time from peak gape until closure of the jaws. Events occurring after the mouth closes are considered to occur in the *recovery* phase.

An important result of the electromyographic data is that all 11 cranial muscles studied initiate electrical activity on average within 0.34 msec of each other (Fig. 14). There is thus extensive overlap between antagonistic muscles during the expansive phase, and the kinematic pattern is not an accurate predictor of the sequence of onset of cranial muscles. The degree of overlap in the onset of muscle activity for the ambystomatids studied here is greater than that found previously in fishes with comparably rapid strikes. Bone movement is also delayed significantly beyond the onset of muscle activity, and the first detectable movements usually occur 15 msec after the first activity in the depressor mandibulae (e.g., Fig. 13). By the time peak gape has been reached (37.4 msec on average; Fig. 12), electrical activity in both the depressor mandibulae and adductor mandibulae muscles has peaked and the amplitude of electrical activity in these muscles varies from 70% (internal adductor) to 30% (depressor mandibulae) of peak amplitude. During the last half of the compressive phase, there is little muscle activity. This can be attributed to the delay in the decay of tension in muscle fibers after the cessation of stimulation.

During the recovery phase, the intermandibularis posterior and coracomandibularis are active (Fig. 14). Contraction of these muscles is associated with the slow compression of the buccal cavity following mouth closure and the last stages of water flow out over the gill apparatus. As noted in the Results section, the coracomandibularis can adduct or abduct the mandible depending on the extent of antagonistic activity in the jaw adductors. During the compressive and recovery phases, when there is still tension in the adductors, coracomandibularis contraction will result in buccal compression.

An additional important feature of the strike is the congruence of the period of greatest stereotypy in different cranial muscles as indicated by the coefficients of variation (Fig. 15). With the sole exception of the internal adductor muscle, which is most stereotyped just prior to maximum gape, all muscles display minimum variability at the start of the expansive phase. This is not an artifact of larger mean amplitudes but reflects a real period of relative stereotypy in EMG spike number and amplitude. As is expected, the variability in kinematic parameters also is lowest at this time (Fig.15). Gans and Gorniak ('82) found that several muscles used in tongue flipping in toads (*Bufo marinus*) showed minimum variation during the protrusion phase, but other studies have not generally reported the periods of minimum variation; as yet no general picture of muscle activity variation during a high-speed strike is possible.

A prominent feature of the electromyogram of the jaw adductor muscles is the relatively low amplitude and low frequency spikes that characterize the onset of activity. A particularly clear example of this is illustrated in Figure 16 (A and B) in which the internal adductor initiates activity with low amplitude spikes that then increase in amplitude and frequency 30 msec later. Not all feedings showed this pattern in the extreme form illustrated in Figure 16, but the delay in maximum spike amplitude and number in the adductor muscles is clearly reflected by the myograms analyzed in Figure 15. Thus, even though the mean differences in onset time of antagonistic muscles such as the depressor mandibulae and adductor mandibulae are very small (less than 0.5 msec), there are consistent and repeatable differences in myogram spike number and amplitude that are concordant with the kinematic pattern.

Models of suction feeding in vertebrates

One of the key elements of recent investigations of suction feeding in fishes has been the use of pressure transducers to measure the pressure inside the mouth cavity during prey capture (Alexander,'69, '70; Liem, '78). Recently, pressure recordings have been used to test critically models of suction feeding hydrodynamics (Lauder, '83a), and recordings of the impedance between adjacent gill bars have provided a preliminary indication of the importance of branchial resistance during feeding (Lauder, '85).

The data presented here for aquatic salamanders extend the generality of this previous work, as simultaneous pressure recordings, electromyograms, and gill impedance measurements are now available for urodeles. Also, because salamanders lack the bony operculum of ray-finned finned fishes, they provide a critical test of the role of the branchial apparatus in the suction feeding mechanism. The key questions addressed here are 1) Do aquatic salamanders show a pattern of gill bar movement during suction feeding similar to that of ray-finned fishes? and 2) Are the pressure recordings and gill bar morphology and function in salamanders consistent with the model of suction feeding in fishes proposed elsewhere (Lauder, '83a,c)?

Figure 16B illustrates clearly that the ceratobranchials undergo a cycle of adduction as the pressure drops followed by abduction as the pressure returns to ambient levels. The analysis of the timing of gill bar (ceratobranchial) movement relative to other events shown in Figure 12 unambiguously indicates that maximum adduction of the branchial apparatus coincides with maximum negative buccal pressure *and* with peak gape. There is no statistically significant difference between the means of these three times with a sample size of N = 20. Maximum abduction of the ceratobranchials occurs much later (mean time to peak abduction is 89.5 msec), and the mouth is nearly closed at this point. The final adduction of the ceratobranchials to reach their initial (rest) position occurs during the recovery phase of the strike (Fig. 16).

These results are entirely consistent with previous data on ray-finned fishes and indicate that the branchial apparatus is functioning as a dynamic resistance within the mouth cavity. Because the process of suction feeding involves a rapid increase in the volume of the mouth cavity as the prey is approached, water will flow into any available opening of the buccal cavity when the pressure drops. These data on the movement of the ceratobranchials in conjunction with morphological evidence provided by the presence of interlocking gill rakers on the gill bars (Fig. 6) indicate that the adduction of the branchial apparatus forms a resistance to water flow that effectively seals off the posterior wall of the mouth during the expansive and early compressive phases of feeding. It is especially noteworthy that maximum branchial adduction coincides precisely with peak negative pressure and maximum gape. Figure 16 also indicates that gill bar adduction begins *after* buccal pressure has begun to drop, and there might thus be a brief period when water flows anteriorly into the mouth cavity from behind the gill bars. This would also be consistent with a proposed brief period of posterior-to-anterior (reverse) flow at the start of mouth opening in fishes (Lauder, '80c) due also to a short (10–40 msec) delay in branchial adduction.

The unidirectional flow of water through the mouth cavity in aquatic ambystomatids is thus a consequence of the functional morphology of the branchial apparatus. The ceratobranchials have a high resistance to flow during the expansive and early compressive phases of feeding and a relatively low resistance to flow as the mouth closes and water flows posteriorly between the ceratobranchials and exits from the buccal cavity.

This pattern is virtually identical to that described previously for ray-finned fishes (Lauder, '83a). In fishes, the branchial apparatus also acts as a dynamic resistance, with adduction of the ceratobranchials occurring as the mouth opens and abduction starting during the compressive phase. In ray-finned fishes, however, the branchial apparatus divides the mouth cavity into buccal and opercular chambers, whereas in aquatic salamanders the branchial apparatus forms the posterior wall of the mouth cavity. These results thus extend to urodeles the basic role of the branchial apparatus as a resistance, first proposed for ray-finned fishes, and demonstrate the generality of the gill resistance and its importance in suction feeding. The operculum of ray-finned fishes is commonly believed to prevent water influx at the back of the head during the strike (e.g., Osse, '69), but such a function has been disproved (Lauder, '83a,c), and the dominant functions of the operculum in the head of ray-finned fishes are 1) its role as a mechanical link in the mechanism of mouth opening and 2) its role in the opercular suction pump during respiration. Thus the function of the branchial resistance in the feeding mechanism of urodeles and fishes is directly comparable.

One final aspect of the data presented in this paper that is relevant to suction feeding are the results of the multiple regression analyses. A comparison of the results shown in Table 4 (model D, the full model) and Table 2 (onset and offset variables) shows that the ability of electromyographic variables to predict variation in some dependent variable is much greater when pressure variables are

used as dependent variables than when kinematic patterns are used. For example, Table 2 shows that EMG data analyzed for the onset and offset of muscle activity explains on average 27% of the variance in any kinematic parameter. On the other hand, if EMG onsets and offsets are used to predict variation in any aspect of the negative pressure generated within the mouth cavity, nearly 61% of the variation in the dependent (pressure) variable is explained. This result might be due to the fact that pressures within the mouth cavity provide a better measure of overall feeding performance than any one kinematic variable alone, because pressure decreases are the net result of integrated muscle activity and bone movement in all the functional units of the head. This suggests that mouth cavity pressures, and especially integrated pressure (or impulse), provide the best quantitative measure of feeding performance for comparative analyses of feeding in salamanders with different head morphologies and for studies of how the type of prey eaten affects feeding behavior. On a broader scale, integrated (negative) buccal pressure, a measure of the *impulse* or change in momentum of the water moved during the strike (Rouse, '78), promises to serve as a useful standard by which to compare suction feeding vertebrates with different anatomical designs (e.g., ray-finned fishes, salamanders, and turtles). Different head morphologies, mouth areas and volumes, and the speed of the strike all contribute to the value of fluid impulse. A comparison of impulse values for different species promises to provide a meaningful (and easily obtained) measure of suction feeding ability or performance.

The pressures generated during suction feeding by aquatic ambystomatid salamanders are lower by roughly an order of magnitude than those measured for ray-finned fishes, and yet the durations of the negative pressure phase appear to be comparable. Precise comparisons of impulse values for ray-finned fishes and salamanders have not yet been made, but preliminary data suggest that an ambystomatid salamander of similar head length to a percomorph fish such as a sunfish will generate 10–100 times less momentum change in the water during feeding. The anatomical and functional bases of this difference remain to be assessed.

Muscles and movements

The third goal of this paper is to use the data gathered on the functional morphology of aquatic prey capture in ambystomatid salamanders to test the value of alternative methods of analyzing electromyographic data. By using three different methods of summarizing EMG data (onsets and offsets of muscle activity, mean amplitude of EMG spikes per unit time interval, and mean EMG spike number times amplitude per unit time interval) to predict variation in kinematic variables, it is possible to assess the relative abilities of the three analytical methods to predict movement patterns. The results indicate unambiguously that EMG amplitude alone is inferior to EMG data analyzed for spike number *and* spike amplitude (Table 2). In fact, considerations of EMG spike amplitude alone appear to provide no more information about the movement pattern than onset and offset analyses. Thus the frequency of spikes within a myogram is of considerable importance in explaining variation in movement patterns. It should be emphasized that this is true even though three of the kinematic variables measured the maximum excursion of a bone or bones (e.g., peak head lift) and thus might be expected a priori to correlate well with EMG amplitude. This was not the case. Similarly, "onset-offset" analyses might be expected to be best at predicting variables that measure the time taken for a movement to occur, because no amplitude information is derived from the myogram; such was not the case.

It is important to note that, because we are using residual variance about the regression to evaluate competing models and are *not* testing hypotheses about regression lines per se, it is not necessary that the standard parametric assumptions of regression analyses be met. The functional form of the relationship between variables should be roughly equivalent in all models, however, and in all cases that we examined using bivariate scatterplots this was true.

Although the "spike number times amplitude" method of analyzing myograms was not statistically significantly better than "onset-offset" analysis (Table 2) at predicting kinematic variables, we again emphasize that with only seven kinematic variables available this is a relatively weak test for rejecting our null hypothesis. The major trend in the data indicates that the "spike number times amplitude" method is in fact a superior predictor of kinematic variance. The "onset-offset" technique only produced a higher R^2 value two of seven times. Also, the mean amount of variance explained by the "onset-offset" approach was 26%; the

"spike number times amplitude" method averaged nearly 40%.

The nature of these results might be a consequence of the high-speed of prey capture in ambystomatid salamanders. When the major components of the movement pattern occur in less than 100 msec, differences between muscles in onset and offset times might not be as relevant to predicting movements as in cases in which movements typically last several seconds. Comparable analyses of slow movements (such as terrestrial locomotion) may result in higher R^2 values for "onset-offset" methods than those obtained here.

In summary, if the three techniques are ranked as to their ability to predict the kinematic pattern, then the "spike number times amplitude" method emerges first, followed by "onset-offset" methods and by "spike amplitude" techniques. The "spike number times amplitude" method is thus recommended if myograms are used to explain movement patterns. This analysis emphasizes the importance of comparing different analytical approaches to the information content of electromyograms and the value of progressing beyond qualitative approaches to EMG duration and amplitude with no statistical basis or quantitative support (e.g., Sibbing, '82).

Evolution of lower vertebrate feeding mechanisms

The comparative functional analyses of lower vertebrate feeding mechanisms completed over the last 5 years have begun to reveal new patterns and have permitted new generalizations about vertebrate evolution. One of the most striking aspects of this pattern is the high level of functional conservatism among aquatic feeding systems: All clades that have been examined to date (ray-finned fishes, coelacanths, lungfishes, and urodeles) share several functional and structural characteristics. Four features are of special importance in the aquatic feeding mechanism of lower vertebrates.

First, a key biomechanical pathway mediating lower jaw depression involves the hypaxial muscles, the rectus cervicis, hyoid apparatus, and the mandibulohyoid ligament. As has been documented elsewhere (e.g., Lauder, '80a,b), posteroventral movement of the hyoid results in mandibular depression. The extreme phylogenetic conservatism of this pathway is demonstrated by its widespread (and primitive) presence in elasmobranchiomorphs, ray-finned fishes, coelacanths, lungfishes, and aquatic salamanders. Many terrestrial salamanders (e.g., plethodontids, Lombard and Wake, '77, Fig. 18) retain the mandibulohyoid ligament, but it extends anteroventrally from its origin on the mandible due to the anterior location of the hyoid. This feature of the feeding mechanism has thus been retained for over 400 million years of vertebrate history.

Second, the kinematic pattern at the strike displays a consistent pattern in all clades studied experimentally: Peak hyoid depression and cranial elevation are achieved after maximum gape. In ray-finned fishes, peak gape, hyoid depression, and opercular abduction occur in a well defined anterior-to-posterior sequence that contributes to the unidirectional flow of water through the buccal cavity.

Third, the mechanism of suction feeding in all clades is similar, with the hyoid apparatus providing the major change in buccal volume during suction feeding. Rotation of the hyoid posteroventrally causes a large increase in volume of the buccal cavity that results in a flow of water (and the prey item) into the mouth.

Fourth, the pattern of water flow during suction feeding is unidirectional, in an anterior-to-posterior direction, and this is due to a variable gill resistance preventing water influx at the back of the head as the mouth is opened. In salamanders and fishes, the branchial apparatus functions as a dynamic resistance: Gill bar adduction and interlocking gill rakers result in high resistance during the expansive phase, and subsequent abduction of the ceratobranchials greatly reduces the resistance allowing water to flow posteriorly out of the mouth.

The range of comparative data on fishes and amphibians now available permits a reassessment of F.H. Edgeworth's classic paper "On the muscles used in shutting and opening the mouth" ('31). In that paper, Edgeworth attempted to trace the phylogenetic patterns of mandibular depressing and elevating mechanisms in vertebrates. He suggested that the primitive mechanism of mandibular depression in vertebrates involved the rectus cervicis and geniohyoideus muscles, a conclusion that can be substantiated at least in part today. However, Edgeworth makes no mention of the mandibulohyoid ligament or of the mechanism by which the hyoid apparatus effects mandibular depression. Experimental work has also shown that the rectus cervicis (= sternohyoideus) is relatively ineffective in mediating mandibular depression in the absence of syn-

chronous activity in the hypaxial muscles. The hypaxial musculature is important in stabilizing the pectoral girdle and in providing a reasonably stable origin for the rectus cervicis. The phylogenetic patterns to mouth-opening mechanisms in lower vertebrates (as currently understood) can be summarized as follows. Primitively in teleostomes, the mouth is opened by two systems: elevation of the cranium by the epaxial muscles and depression of the mandible by the rectus cervicis (= sternohyoideus) via the hyoid and mandibulohyoid ligament. In primitive ray-finned fishes (e.g., *Polypterus* of *Lepisosteus* these are the *only* mechanisms for opening the mouth. These two systems have been inferred to occur in coelacanths (Lauder, '80b), and both these systems are present in lungfishes along with an additional one: mandibular depression via the depressor mandibulae muscle. Edgeworth ('31) is in error when he reports that "depression of the jaw in Dipnoi and Elasmobranchii is effected by the genio-coracoideus or geniothoracicus . . ."; these muscles have not been shown to contribute to mouth opening (Bemis and Lauder, '85). Larval urodeles appear to share the same three mouth-opening and closing mechanisms as lungfishes, although the homology of the depressor mandibulae muscle in the two groups is disputed. In sum, the amniote feeding mechanism is based on a fundamentally conservative biomechanical system with three general components involved in opening and closing the mouth: the epaxial muscles, the hyoid apparatus, and the depressor mandibulae.

Perhaps the most critical question that remains to be answered is the reason for these conservative kinematic and morphological patterns. Are the conservative features in the feeding mechanism of these clades simply a consequence of the density and viscosity of water as a medium from which food must be extracted (Bramble, '73)? In other words, are the functional constraints on the process of aquatic food capture so high that there is only one solution to the problem of capturing prey by suction feeding? Alternatively, the feeding mechanism might represent a primitive system that, once evolved, has simply never changed. To answer this question, it will be necessary to expand our understanding of the process of food capture to situations in which a direct comparison can be made of terrestrial and aquatic prey-capture methods. Approaches to this question of constraints on the aquatic feeding mechanism in lower vertebrates can be discussed within a framework of four avenues for future research.

1) What functional changes occur in the transition from an aquatic to a terrestrial feeding method? Surprisingly little attention has been paid to the transition from aquatic to terrestrial feeding and to the differing constraints imparted by air and water on the functional morphology of prey capture (see Bramble and Wake, '85, for an overview of this problem). Two systems in particular would serve to answer this question. First, the function of the head could be studied in individual salamanders from the aquatic larval stage through metamorphosis. Second, terrestrial salamanders that return to the water to breed and feed (Ozeti and Wake, '69) could be studied to determine whether or not secondarily aquatic feeding mode is similar in pattern to the larval pattern in other aquatic salamanders. Does the kinematic pattern at the strike differ when a metamorphosed salamander returns to the water to feed? If differences were found (between larval salamanders and those individuals that return to the water after metamorphosis) in the timing of hyoid movement, and other aspects of the basic feeding mechanism remained similar, for example, then the hypothesis that there is only one, highly constrained, method of suction feeding would be falsified.

An additional important area in this context is the transformation of the role of the hyoid apparatus from a dominant functional component in suction feeding to a food gathering and processing system (Bramble and Wake, '85; Gans and Gorniak, '82; Larson and Guthrie, '75). Reorganization of hyoid osteology and myology during metamorphosis might radically alter the timing of head movements at the strike and the activity patterns of head muscles in both terrestrial and aquatic feeding. An analysis of secondarily aquatic salamanders would prove particularly useful; there is not a major anatomical reorganization of the head during this ecological transition.

2) Are there differences in the function of unidirectional and bidirectional feeding systems? Despite considerable progress in our understanding of the hydrodynamics of suction feeding, we have no data that bear on perhaps the most general distinction among aquatic feeding mechanisms: the difference between feeding systems in which water flow is unidirectional (in the mouth and out

through a gill opening posteriorly), and those (such as in turtles) in which water that enters the mouth during the strike is subsequently expelled back through the mouth anteriorly (bidirectional flow).

3) Does the type of prey eaten change the pattern of aquatic prey capture in salamanders? We have barely begun to address the diversity of aquatic feeding modes in salamanders, and this study has focused only on the capture of one prey type, worms. An important next step will be to quantify the extent of plasticity in the feeding mechanism in response to different prey types.

4) Do other clades that remain to be examined in detail (sharks and turtles) show patterns similar to those of fishes and salamanders? If the patterns presently believed to be general ones in lower vertebrates are also true of sharks and aquatic turtles, then a firm historical basis will have been established for the consideration of functional design in amniote feeding mechanisms.

ACKNOWLEDGMENTS

This research was supported by grants from the National Science Foundation (PCM 81-21649), the Block Fund (University of Chicago), the A. Mellon Foundation, the Eli A. Nierman Fund (University of Chicago), and an NIH training grant (Genetics and Regulation). In addition, the Whitehall Foundation provided essential support to G.V.L. for the computer equipment and programming. NSF grant BSR 81-15048 supported the research on functional design and evolution of ray-finned fishes cited here. We thank S. Barghusen for data analysis and for maintaining the animals during the experiments. C. Richardson drew the anatomical figures. We especially thank C. Smither for superb computer programming. We are grateful to C. Gans, W. Bemis, R.E. Lombard, P. Wainwright, S. Emerson, B. Clark, S. Herring, and anonymous reviewers for helpful discussions and/or comments on the manuscript.

LITERATURE CITED

Alexander, R.McN. (1969) Mechanics of the feeding action of a cyprinid fish. J. Zool. (London) *159:*1–15.

Alexander, R.McN. (1970) Mechanics of the feeding action of various teleost fishes. J. Zool. (London) *162:*145–156.

Allis, E.P. (1917) Homologies of the muscles related to the visceral arches of the gnathostome fishes. Q. J. Microsc. Sci. *62:*303–406.

Beach, J., G.C. Gorniak, and C. Gans (1982) A method for quantifying electromyograms. J. Biomechanics *15:*611–617.

Bemis, W.E., K. Schwenk, and M.H. Wake (1983) Morphology and function of the feeding apparatus in *Dermophis mexicanus* (Amphibia: Gymnophiona). Zool. J. Linn. Soc. *77:*75–96.

Bemis, W., and G.V. Lauder (1985) Morphology and function of the feeding apparatus of the lungfish, *Lepidosiren paradoxa* (Dipnoi). J. Morphol. (in press).

Bramble, D.M. (1973) Media dependent feeding in turtles. Am. Zool. *13:*1342.

Bramble, D.M., and D.B. Wake (1985) The feeding mechanisms of lower tetrapods. In M. Hildebrand, D. Wake, K. Liem, and D. Bramble (eds): Functional Vertebrate Morphology. Cambridge: Harvard University Press.

Carroll, R.L., and R. Holmes (1980) The skull and jaw musculature as guides to the ancestry of salamanders. Zool. J. Linn. Soc. *68:*1–40.

Crompton, A.W., and P. Parker (1978) Evolution of the mammalian masticatory apparatus. Am. Sci. *66:*192–201.

Dalrymple, G.H., J.E. Juterbock, and A.L. La Valley (1985) Function of the atlanto-mandibular ligaments of desmognathine salamanders. Copeia *1985:*254–257.

Dingerkus, G., and L.D. Uhler (1977) Enzyme clearing of alcian blue stained whole small vertebrates for demonstration of cartilage. Stain Technol. *52:*229–232.

Druner, L. (1901) Studien zur Anatomie der Zungenbein-, Kiemenbogen- und Kehlkopfmuskelen der Urodelen. I. Theil. Zool. Jahrbl. Anat. *15:*435–622.

Eaton, T.H. (1936) The myology of salamanders with particular reference to *Dicamptodon ensatus* (Eschscholtz). J. Morphol. *60:*31–75.

Edgeworth, F.H. (1911) On the morphology of the cranial muscles in some vertebrates. Q. J. Miscrosc. Sci. *56:*167–316.

Edgeworth, F.H. (1931) On the muscles used in shutting and opening the mouth. Proc. Zool. Soc. Lond. *3:*817–818.

Edgeworth, F.H. (1935) The Cranial Muscles of Vertebrates. Cambridge: Cambridge University Press.

Erdman, S., and D. Cundall (1984) The feeding apparatus of the salamander *Amphiuma tridactylum:* Morphology and behavior. J. Morphol. *181:*175–204.

Gans, C., and G. C. Gorniak (1982) Functional morphology of lingual protrusion in marine toads (*Bufo marinus*). Am. J. Anat. *163:*195–222.

Gans, C., and R.G. Northcutt (1983) Neural crest and the origin of vertebrates: A new head. Science *220:*268–274.

Gaupp, E. (1904) Das Hyobranchialskelett der Wirbeltiere. Ergeb. Anat. Entw. Gesch. 14.

Gorniak, G.C., H.I. Rosenberg, and C. Gans (1982) Mastication in the Tuatara, *Sphenodon punctatus* (Reptilia: Rhynchocephalia): Structure and activity of the motor system. J. Morphol. *171:*321–353.

Huxley, T.H. (1864) Lectures on the elements of comparative anatomy. London.

Jarvik, E. (1963) The composition of the intermandibular division of the head in fish and tetrapods and the diphyletic origin of the tetrapod tongue. Kungl. Sven., Vet. Hand. *9:*1–74.

Keller, R. (1946) Morphogenetische Untersuchungen am Skelett von *Siredon mexicanus* Shaw mit besonderer Berucksichtigung des Ossifikationsmodus beim neotenen Axolotl. Rev. Suisse Zool. *53:*329–426.

Krogh, J.E., and W.W. Tanner (1972) The hyobranchium and throat myology of the adult Ambystomatidae of the United States and Northern Mexico. Brigham Young Univ. Sci. Bull. Biol. Ser. *16:*1–69.

Larson, J.H., and D.J. Guthrie (1975) The feeding system of terrestrial Tiger Salamanders (*Ambystoma tigrinum melanostictum* Baird). J. Morphol. *147:*137–154.

Lauder, G.V. (1980a) Evolution of the feeding mechanism in primitive actinopterygian fishes: A functional

anatomical analysis of *Polypterus, Lepisosteus*, and *Amia*. J. Morphol. *163*:283–317.
Lauder, G.V. (1980b) The role of the hyoid apparatus in the feeding mechanism of the living coelacanth, *Latimeria chalumnae*. Copeia *1980*:1–9.
Lauder, G.V. (1980c) Hydrodynamics of prey capture in teleost fishes. In D. Schneck (ed.): Biofluid Mechanics. New York: Plenum Press, pp. 161–181.
Lauder, G.V. (1982) Patterns of evolution in the feeding mechanism of actinopterygian fishes. Am. Zool. *22*:275–285.
Lauder, G.V. (1983a) Prey capture hydrodynamics in fishes: experimental tests of two models. J. Exp. Biol. *104*:1–13.
Lauder, G.V. (1983b) Functional and morphological bases of trophic specialization in sunfishes (Teleostei, Centrarchidae). J. Morphol. *178*:1–21.
Lauder, G.V. (1983c) Food capture. In P.W. Webb and D. Weihs (eds): Fish Biomechanics. New York: Praeger Publishers, pp. 280–311.
Lauder, G.V. (1985) Functional morphology of the feeding mechanism in lower vertebrates. In H.-R. Duncker and G. Fleischer (eds): Functional Morphology of Vertebrates. New York: Springer Verlag.
Liem, K.F. (1978) Modulatory multiplicity in the functional repertoire of the feeding mechanism in cichlid fishes. I. Piscivores. J. Morphol. *158*:323–360.
Lombard, R.E., and D.B. Wake (1976) Tongue evolution in the lungless salamanders, Family Plethodontidae. I. Introduction, theory and a general model of dynamics. J. Morphol. *148*:265–286.
Lombard, R.E., and D.B. Wake (1977) Tongue evolution in the lungless salamanders, Family Plethodontidae. II. Function and evolutionary diversity. J. Morphol. *153*:39–80.
Luther, A. (1914) Uber die vom N. trigeminus versorgte Muskulatur der Amphibien. Acta Soc. Sci. Fenn. *44*:1–151.
Mallatt, J. (1984a) Early vertebrate evolution: pharyngeal structure and the origin of gnathostomes. J. Zool. (London) *204*:169–183.
Mallatt, J. (1984b) Feeding ecology of the earliest vertebrates. Zool. J. Linn. Soc. Lond. *82*:261–272.
Marche, C., and J.P. Durand (1983) Recherches comparatives sur l'ontogenese et l'evolution de l'appareil hyobranchial de *Proteus anguinus* L., proteidae aveugle des eaux souterraines. Amphibia-Reptilia *4*:1–16.
Matthes, E. (1934) Bau und Function der Lippensaume wasserlebender Urodelen. Z. Morphol. Okol. Tiere *28*:155–169.
Osse, J. (1969) Functional morphology of the head of the perch (*Perca fluviatilis L.*): An electromyographic study. Neth. J. Zool. *19*:289–392.
Ozeti, N., and D.B. Wake (1969) The morphology and evolution of the tongue and associated structures in salamanders and newts (Family Salamandridae). Copeia *1969*:91–123.
Piatt, J. (1938) Morphogenesis of the cranial muscles of *Amblystoma punctatum*. J. Morphol. *63*:531–587.
Piatt, J. (1939) Correct terminology in salamander myology I. Intrinsic gill musculature. Copeia *1939*:220–224.
Piatt, J. (1940) Correct terminology in salamander myology II. Transverse ventral throat musculature. Copeia *1940*:9–14.
Roth, G. (1976) Experimental analysis of the prey catching behavior of *Hydromantes italicus* Dunn (Amphibia, Plethodontidae). J. Comp. Physiol. *109*:47–58.
Rouse, H. (1978) Elementary Mechanics of Fluids. New York: Dover.,
Severtzov, A.S. (1968) The evolution of the hyobranchial apparatus in the larvae of amphibia. Smithsonian Herp. Info. Serv. *21*:1–8 (translated from the Russian).
Shaffer, H.B. (1984) Evolution in a highly paedomorphic lineage. I. An electrophoretic analysis of the Mexican Ambystomatidae. Evolution *38*:1194–1206.
Shaffer, H.B., and G.V. Lauder (1985a) Aquatic prey capture in ambystomatid salamanders: Patterns of variation in muscle activity. J. Morphol. *183*:273–284.
Shaffer, H.B., G.V. Lauder (1985b) Patterns of variation in aquatic ambystomatid salamanders: Kinematics of the feeding mechanism. Evolution *39*:83–92.
Sibbing, F. (1982) Pharyngeal mastication and food transport in the carp (*Cyprinus carpio* L.): A cineradiographic and electromyographic study. J. Morphol. *172*:223–258.
Siegel, S. (1956) Non-Parametric Statistics for the Behavioral Sciences. New York: McGraw Hill.
Sokal, R., and F.J. Rohlf (1981) Biometry. San Francisco: W.H. Freeman.
Thexton, A.J., D.B. Wake, and M.H. Wake (1977) Tongue function in the salamander *Bolitoglossa occidentalis*. Arch. Oral Biol. *22*:361–366.
Valentine, B.D., and D.M. Dennis (1964) A comparison of the gill-arch system and fins of three genera of larval salamanders, *Rhyacotriton, Gyrinophilus*, and *Ambystoma*. Copeia *1964*:196–201.
Vetter, B. (1874) Untersuchungen zur vergleichenden Anatomie der Kiemenund Kiefermuskulatur der Fische. I. Selachien. Zeitschr. Bd. (Jena) *8*:405–458.
Wake, D.B. (1982) Functional and developmental constraints and opportunities in the evolution of feeding systems in urodeles. In D. Mossakowski and G. Roth (eds): Environmental Adaptation and Evolution. Stuttgart: Gustav Fischer, pp. 51–66.
Walker, W.F. (1975) Vertebrate Dissection, 5th ed. Philadelphia: W.B. Saunders.
Weijs, W.A., and R. Dantuma (1981) Functional anatomy of the masticatory apparatus in the rabbit (*Oryctolagus cuniculus* L.). Neth. J. Zool. *31*:99–147.